

Evaluating Coastal Wetland Restoration in Louisiana Using Drones

A Thesis

Presented to the

Graduate Faculty of the

University of Louisiana at Lafayette

In Partial Fulfillment of the

Requirements for the Degree

Master of Science

J. Mason Harris

Summer 2020

© J. Mason Harris

2020

All Rights Reserved

Evaluating Coastal Wetland Restoration in Louisiana Using Drones

J. Mason Harris

APPROVED:

James Nelson, Chair
Assistant Professor of Biology

Kelly L. Robinson
Assistant Professor of Biology

Mark Hester
Professor of Biology

Whitney Broussard III
Senior Scientist at JESCO, Inc.

Glenn M. Suir
Research Agronomist at U.S. Army
Engineer Research and Development
Center

Mary Farmer-Kaiser
Dean of the Graduate School

Acknowledgements

I would like to thank my advisor, Dr. James Nelson, for giving me the opportunity to earn a master's degree and for providing his guidance throughout my time at ULL. I am also grateful to Louisiana Sea Grant for supporting me and providing funding to make this project possible. I would like to specifically thank Dani Dilullo and Dr. Robert Twilley from LA Sea Grant.

I thank my committee members for their scientific expertise and advice throughout the thesis development process. Dr. Whitney Broussard III, Dr. Glenn Suir, Dr. Kelly Robinson, and Dr. Mark Hester were all instrumental in providing guidance on geospatial and ecological principles. My lab members Ryan James, Justin Lesser, David Behringer, Skylar Flaska, and Kristen Fellows made data collection possible and supplied insights and suggestions during the project. Grant Lafleur was also instrumental in helping with field work. The U.S. Fish and Wildlife Service (USFWS) provided access to the Sabine National Wildlife Refuge. I would like to thank Terry Delaine from the USFWS for his help as the Sabine Refuge Manager.

Finally, I would like to thank my wife, Susan, for her endless love and support. She has always been there for me and constantly encouraged my passions.

Table of Contents

Acknowledgements	iv
List of Tables	vi
List of Figures	vii
List of Abbreviations	ix
Chapter 1: General Introduction	1
Wetlands and Coastal Louisiana	1
Research Approach	3
Objectives	5
References	7
Chapter 2: Evaluating Coastal Wetland Restoration In Louisiana Using Drones	9
Introduction	9
Methods	14
Study sites.	14
Planning and field work.	17
Processing and analysis.	20
Results	28
Discussion	32
Tables	42
Figures	55
References	75
Abstract	81
Biographical Sketch	82

List of Tables

Table 2.1. Plant species surveyed in restored and reference sites at the refuge.....	42
Table 2.2. Land and water interface results	43
Table 2.3. Land and water calculations from drone imagery (June/July 2019), color infrared aerial photographs (7 December 2015), and WorldView-3 satellite imagery (13 February 2016).....	44
Table 2.4. 2019 Drone-based edge habitat calculations (marsh to water border	45
Table 2.5. Landscape metrics for land and water classes (water rows shown in gray	46
Table 2.6. Landscape metrics for Cycle 2 run separately for the area within the original containment dikes and the overflow area (refer to figure 2.2 for delineation.....	47
Table 2.7. Class area statistics for 2019 drone-based classifications.....	48
Table 2.8. Cycle 5 accuracy assessment (confusion) matrix results	49
Table 2.9. Cycle 2 accuracy assessment (confusion) matrix results	50
Table 2.10. Cycle 3 accuracy assessment (confusion) matrix results	51
Table 2.11. Cycle 1 accuracy assessment (confusion) matrix results	52
Table 2.12. Reference North accuracy assessment (confusion) matrix results	53
Table 2.13. Reference South accuracy assessment (confusion) matrix results	54

List of Figures

Figure 2.1. Location of study sites (Cycles) with final construction year in the Sabine National Wildlife Refuge (Bing 2017 base map).....	55
Figure 2.2. Field sampling locations and flight areas covered by the Yuneec H520. Examples of vegetation include: a mixture of <i>Spartina alterniflora</i> , <i>Schoenoplectus robustus</i> , and <i>Distichlis spicata</i> in the foreground with taller <i>Phragmites australis</i> in the background (a) and <i>Spartina alterniflora</i> (b).....	56
Figure 2.3. Data products from June 2019 drone imagery for Cycle 3 including: orthomosaic (a), digital surface model (b), land water interface (c), and vegetation classification (d).....	57
Figure 2.4. Workflow for obtaining, processing, and analyzing drone imagery	58
Figure 2.5. Example of <i>Spartina patens</i> marsh illustrating an aggregated piece of habitat (a) (AI = 100) and a less aggregated piece of habitat (b) (AI = 99	59
Figure 2.6. Summer 2019 drone-based percent land cover for restored sites over time since restoration (gray area is 95% confidence interval for logarithmic line	60
Figure 2.7. Summer 2019 drone-based land and water interface maps (years since construction as of 2019) (Bing 2017 base map).....	61
Figure 2.8. Summer 2019 drone-based vegetation classification maps (years since construction as of 2019) (Bing 2017 base map).....	62
Figure 2.9. Drone-based percent cover calculations by species and land cover class	63
Figure 2.10. July 2019 Cycle 5 (4 years old) orthomosaic (a) with zoomed in portions (b) and corresponding classifications (c).....	64
Figure 2.11. July 2019 Cycle 2 (9 years old) orthomosaic (a) with zoomed in view of the overflow area (b) and corresponding classification (c) to highlight the detail of drone products and the tidal channels and edge habitat created by the overflow technique	65
Figure 2.12. June 2019 Cycle 3 (12 years old) orthomosaic (a) and classification (b) with zoomed in view of the flooded portion (c) and corresponding classification (d)	66
Figure 2.13. June 2019 Cycle 1 (17 years old) orthomosaic (a) and corresponding classification map (b) with zoomed in portions highlighting <i>Phragmites australis</i> (c) and portion of man-made channel filling in (d)	67

Figure 2.14. June 2019 Reference North orthomosaic (a) with corresponding classification (b) and Reference South orthomosaic (c) with corresponding classification (d).....68

Figure 2.15. 2019 field-based percent vegetation cover estimates69

Figure 2.16. Field-based species richness (a) (# species per plot) (ANOVA, $F_{5,49} = 2.01$, $P = .0941$) and average percent vegetated cover estimates (b) (ANOVA, $F_{5,49} = 6.28$, $P = .0001$).....70

Figure 2.17. 2019 field-based Floristic Quality Index (FQI) scores71

Figure 2.18. Dominant cover type comparison of 2018 state agency field surveys (Agency) and 2019 drone-based classifications (Drone) and field surveys (Field). Classes grouped into high marsh (*D. spicata* and *S. patens*), low marsh (*S. alterniflora*), and other (all other species) for general comparison across data types. Agency and Field columns based on visual percent cover estimates from plot surveys.....72

Figure 2.19. Standardized edge habitat comparison (edge considered marsh to water border)73

Figure 2.20. Orthomosaic (left) and corresponding vegetation classification (right) at study sites: Cycle 3 (a), Cycle 2 (b), Reference North (c), and Reference South (d).....74

List of Abbreviations

CPRA	Coastal Protection and Restoration Authority
CRMS	Coastwide Reference Monitoring System
CST	Central Standard Time
CWPPRA	Coastal Wetlands Planning, Protection and Restoration Act
DSM	Digital Surface Model
FQI	Floristic Quality Index
GCP	Ground Control Point
GIS	Geographic Information Systems
GPS	Global Positioning System
JPEG	Joint Photographic Experts Group
LiDAR	Light Detection and Ranging
MTP	Manual Tie Point
RGB	Red, Green, Blue (true color imagery)
SfM	Structure from Motion
SNWR	Sabine National Wildlife Refuge
UAS	Unmanned Aircraft System
ULL	University of Louisiana Lafayette
USFWS	United States Fish and Wildlife Service
USGS	United States Geological Survey

Chapter 1: General Introduction

Wetlands and Coastal Louisiana

Wetlands are some of the most indispensable ecosystems on the planet. The unique environments are widely recognized for supporting fish and wildlife production and maintaining biodiversity. Wetlands are also the filters and regulators of water on the landscape because they are the downstream receivers that absorb pollution, temporarily store floodwaters, and recharge groundwater aquifers (Mitsch & Gosselink 2015). Carbon sequestration in wetlands is also an essential function to mitigate effects of greenhouse gases and global climate change. Although wetlands cover only 5-8% of terrestrial environments, they contain 20-30% of the earth's soil pool of carbon (Mitsch et al. 2013). Wetlands benefit many organisms but also many other habitats. They are transition zones between aquatic and terrestrial environments, otherwise known as an ecotone, that help regulate water quality, exchange nutrients, and protect shorelines.

Coastal estuaries and marshes provide economic and societal benefits like buffering storm impacts, supporting commercial fisheries, and promoting recreation and tourism (Barbier et al. 2011). In 2010, 39% of Americans (123 million people) lived in coastal counties which comprise less than 10% of the total land area in the United States (Crosset et al. 2013). And this was expected to increase 8% (10 million people) by 2020. Coastal societies and economies need healthy intact wetlands to protect valuable fisheries, port facilities, tourist destinations, and fossil fuel resources. Coastal wetlands in the U.S. were calculated to contribute \$23.2 billion per year in storm protection and a loss of 1 hectare of wetland can lead to a \$33,000 increase in damage from individual storms (Costanza et al. 2008). Despite some marshes showing signs of resiliency, many coastal wetlands are facing

major global threats as a result of man's activities and climate related impacts (Millennium Ecosystem Assessment 2005).

Louisiana's coast is an important natural resource that supports cultures, businesses, and ecosystems. Marshes make up much of the coastal habitat but are disappearing rapidly. Louisiana's coastal zone has lost approximately 4,830 square kilometers of wetlands from the 1930's to 2016 (Couvillion et al. 2017). Since roughly 40% of coastal wetlands in the U.S. are found in Louisiana, this loss accounts for 80% of the national reduction in wetlands in the last century (Boesch et al. 1994). The accelerated loss in Louisiana, however, is caused by a combination of factors including Mississippi River levees, oil and gas exploration, channel construction, subsidence, and sea level rise.

Remote sensing is the science of monitoring an area or phenomena from a distance, commonly using aircrafts or satellites, and its practice has been critical for quantifying Louisiana's land loss. Couvillion et al. 2011 analyzed coastal changes over an 80-year period by conducting land and water classifications with survey data, aerial photographs, and Landsat satellite imagery to determine overall land change. Historic rates and trends calculated from land loss maps have been used to estimate future losses and strategize restoration planning (Barras et al. 2003). Remote sensing has also been used to assess coastal damage from major events like hurricanes and oil spills (Barras 2007; Mishra et al. 2012). These techniques are essential since marsh losses are occurring at a coastwide scale and field measurements alone would be logistically impractical.

Due to the rapid loss of these valuable areas, the state is conducting \$50 billion worth of restoration projects to create new habitats and rehabilitate degraded ones (CPRA 2017). A variety of techniques have been employed, such as marsh creation, barrier island restoration,

shoreline protection, terracing, diversions, and hydrologic restoration. The Coastal Protection and Restoration Authority's (CPRA) 2017 Coastal Master Plan currently includes the nation's largest investment in marsh creation at \$17.8 billion over the next 50 years. Since this technique typically consists of creating a new wetland out of a shallow water area, rather than rehabilitating a degraded one, understanding how these areas function as wetland habitats is critical to implementing better restoration techniques in the future.

Research Approach

Off-the-shelf unmanned aircraft systems (UASs), commonly referred to as drones, are being increasingly utilized in environmental assessments. The technology offers monitoring solutions for areas that are difficult to access and greatly benefit from high-resolution maps, like restored coastal wetlands. Traditional methods for monitoring restored wetlands are time and labor intensive and often fail to provide holistic site assessments. Data captured by regular RGB cameras standard with most modern drones can significantly improve our understanding of restoration progress and the development of a site over time. Multispectral, LiDAR, and other precision sensors or cameras are highly beneficial for landscape and vegetation analysis but are not widely available to everyone (Colomina & Molina 2014). Although many studies have used drones and remote sensing to assess wetlands, few have used them specifically for understanding wetland restoration (Zweig et al. 2015; Boon et al. 2016; Husson et al. 2016; Kalacksa et al. 2017; Pande-Chhetri et al. 2017; Broussard et al. 2018; Doughty & Cavanaugh 2019). Drones fill a niche in remote sensing with higher resolutions and greater operational flexibility than manned aircrafts or satellites at a much lower cost, albeit with greatly reduced areal coverage (Klemas 2015). Processing techniques like structure from motion (SfM) photogrammetry can create multiple data types from drone

images, including 3-layer RGB mosaics and digital surface models (DSMs), that can be used to make accurate site maps and vegetation classifications (Husson et al. 2017). The technology is a powerful tool for restoration managers and ultimately provides better knowledge of site development than most traditional surveys.

Field surveys are an essential part of restoration monitoring. They are also necessary to ground truth remote sensing data. Field measurements for restoration monitoring in Louisiana typically include variables like species composition, percent cover, and vegetation height (Folse et al. 2014). Plant identities inform managers on patterns of succession and rates of community change that in theory should ultimately reach some stable, climax ecosystem with a desired suite of plant types. And restoration projects aim to mimic a natural reference area or a pre-existing state using species compositions as a critical metric to determine success. Visual cover estimates, however, are subjective and are often conducted at random stations or along transects that can fail to fully capture a site (Broussard et al. 2018). This ground data, however, can be paired with remote sensing data and used to train software to identify these species at much broader scales.

By combining field surveys and drone imagery, researchers can use holistic site assessments to understand ecological progression and restored function in wetlands. Doughty & Cavanaugh (2019) integrated the two approaches to estimate aboveground biomass in saltmarshes and monitor seasonal changes in productivity. In a restoration context, vegetation classifications and site assessments using principles of landscape ecology will inform development over time. Accurate mapping and spatial analysis of water bodies will help researchers understand site evolution since tidal drainage and channels are important marsh landscape components (Weinstein et al. 2001). Hydrology is also considered the master

variable in structuring plant communities and contributing to overall restoration success and spatial resolution has an impact on mapping of smaller water bodies (Enwright et al. 2014; Mitsch & Gosselink 2015).

Objectives

I combined drone flights and field surveys to understand the ecological sequence of restoration, specifically marsh creation, and integrate more modern tools into coastal wetland evaluation and monitoring. My study area was within the Sabine National Wildlife Refuge in southwest Louisiana. I chose four neighboring restoration projects completed from 2002 – 2015 using a space for time substitution to understand developmental rates. I also picked two natural marshes for reference comparisons. The primary goals of the study were: (1) Develop a workflow to analyze wetland restoration using drones. (2) Understand the sequence of restoration progression and development of wetland plant species. (3) Evaluate the results in terms of the ecology of the sites and compare them to natural reference marshes. (4) Assess the effectiveness of restoration.

Species compositions, land/water ratios, and landscape metrics like edge and fragmentation indices are widely used in remote sensing studies, but their ecological meaning isn't always straightforward and their contribution towards understanding restoration success must be taken into context. A core component of the study was to develop methods to improve wetland restoration assessments and provide managers additional ways to document successes and failures. Based on previous studies, I hypothesized the more mature restoration sites, > 10 years old, would be equivalent to or surpass the reference marshes for percent vegetated cover, species richness, and landscape fragmentation indices. The specific objectives to achieve project goals were as follows: (1) Classify vegetation types at restored

and natural marshes using high-resolution maps, surface models, and field surveys. (2)

Evaluate wetland conditions using landscape ecology metrics and integrate structural analysis with vegetation communities and site “age”. (3) Compare the results across sites and with previous assessments. The cost of restoration itself is high; therefore, it is critical to develop more cost-effective and comprehensive monitoring tools to ensure success and effectively communicate results to stakeholders and policy makers.

References

- Barbier EB et al. (2011) The value of estuarine and coastal ecosystem services. *Ecological Monographs* 81:169–193
- Barras JA et al. (2003) Historical and projected coastal Louisiana land changes: 1978-2050. U.S. Geological Survey. Open-File Report OFR 03-334 (Revised 2004)
- Barras JA (2007) Land area changes in coastal Louisiana after hurricanes Katrina and Rita. In: *Science and the storms: The USGS Response to the Hurricanes of 2005*. Circular 1306 U.S. Geological Survey, Reston, VA pp. 97–112.
- Boesch DF et al. (1994) Scientific assessment of coastal wetland loss, restoration and management in Louisiana. *Journal of Coastal Research Special Issue* 20:1–103
- Boon MA, Greenfield R, Tesfamichael S (2016) Wetland assessment using unmanned aerial vehicle (UAV) photogrammetry. *The International Archives of the Photogrammetry, Remote Sensing and Spatial Information Sciences* XLI-B1:781–788
- Broussard W, Suir G, Visser J (2018) Unmanned Aircraft Systems (UAS) and satellite imagery collections in a coastal intermediate marsh to determine the land-water interface, vegetation types, and normalized difference vegetation index (NDVI) values. U.S. Army Engineer Research and Development Center. ERDC/TN WRAP-18-1, Vicksburg, MS
- Coastal Protection and Restoration Authority of Louisiana (CPRA) (2017) Louisiana's Comprehensive Master Plan for a Sustainable Coast. CPRA, Baton Rouge, LA
- Colomina I, Molina P (2014) Unmanned aerial systems for photogrammetry and remote sensing: A review. *ISPRS Journal of Photogrammetry and Remote Sensing* 92:79–97
- Costanza R et al. (2008) The value of coastal wetlands for hurricane protection. *AMBIO: A Journal of the Human Environment* 37:241–248
- Couvillion BR et al. (2011) Land area change in coastal Louisiana from 1932 to 2010. U.S. Geological Survey. Scientific Investigations Map 3164, Reston, VA
- Couvillion BR et al. (2017) Land area change in coastal Louisiana (1932 to 2016). U.S. Geological Survey. Scientific Investigations Map 3381, Reston, VA
- Crossett K et al. (2013) National coastal population report: Population trends from 1970 to 2020. National Oceanic and Atmospheric Administration
- Doughty CL, Cavanaugh KC Mapping coastal wetland biomass from high resolution unmanned aerial vehicle (UAV) imagery. *Remote Sensing* 11:1–16

- Enwright NM et al. (2014) Analysis of the impact of spatial resolution on land water classifications using high resolution aerial imagery. *International Journal of Remote Sensing* 35:5280–5288
- Folse TM et al. (2014) A standard operating procedures manual for the coastwide reference monitoring system - wetlands: methods for site establishment, data collection, and quality assurance/quality control. Louisiana Coastal Protection and Restoration Authority (CPRA), Baton Rouge, LA
- Husson E, Ecke F, Reese H (2016) Comparison of manual mapping and automated object-based image analysis of non-submerged aquatic vegetation from very-high-resolution UAS images. *Remote Sensing* 8:1–18
- Husson E, Reese H, Ecke F (2017) Combining spectral data and a DSM from UAS-images for improved classification of non-submerged aquatic vegetation. *Remote Sensing* 9:1–15
- Kalacska M et al. (2017) Structure from motion will revolutionize analyses of tidal wetland landscapes. *Remote Sensing of Environment* 199:14–24
- Klemas V (2015) Coastal and environmental remote sensing from unmanned aerial vehicles: An overview. *Journal of Coastal Research* 31:1260–1267
- Millennium Ecosystem Assessment (2005) Millennium ecosystem assessment, Ecosystems and human well-being. World Resources Institute. Island Press, Washington, DC
- Mishra DR et al. (2012) Post-spill state of the marsh: Remote estimation of the ecological impact of the Gulf of Mexico oil spill on Louisiana Salt Marshes. *Remote Sensing of Environment* 118:176–185
- Mitsch WJ et al. (2013) Wetlands, carbon, and climate change. *Landscape Ecology* 28:583–597
- Mitsch WJ, Gosselink JG (2015) *Wetlands*. 5th ed. John Wiley & Sons, Inc., Hoboken, New Jersey
- Pande-Chhetri R et al. (2017) Object-based classification of wetland vegetation using very high-resolution unmanned air system imagery. *European Journal of Remote Sensing* 50:564–576
- Weinstein MP et al. (2001) Restoration principles emerging from one of the world's largest tidal marsh restoration projects. *Wetlands Ecology and Management* 9:387–407
- Zweig C, Burgess MA, Kitchens WM (2015) Use of unmanned aircraft systems to delineate fine-scale wetland vegetation communities. *Wetlands* 35:303–309

Chapter 2: Evaluating Coastal Wetland Restoration in Louisiana Using Drones

Introduction

Restoration is the practice of returning a degraded or destroyed habitat to a previously existing condition or its original state (Bradshaw 1996). Efforts to reach the target state range from rehabilitating specific ecosystem functions or increasing an animal's population to restoring an entire ecosystem (Lake 2001). Ecological restoration implies the intent to restore organisms and the interactions with themselves and the physical environment (Jackson et al. 1995). The approach aims to create the environment necessary for recovery so the plants, animals, and microorganisms can conduct much of the recovery themselves and create a balanced system (Gann et al. 2019). The holistic ecosystem approach has developed over time and relies on self-sustaining populations that require minimal or no additional human intervention. Wetland restoration depends heavily on this concept of self-design and the interactions of specific biotic and abiotic factors like surface elevations, flooding regimes, and plant community structure.

Ecological theory is central to restoration success and can help predict outcomes and track development over time (Zedler 2000). Restoration science is underpinned by several conceptual subdisciplines of ecology like the community assembly theory which suggests that initial restoration success and vegetation establishment can depend on the order of arrival and be guided by structured planting routines (Palmer et al. 1997). Succession is also a key component because a greater understanding of shifting biological communities following restoration actions will inform timelines of site maturity (Young et al. 2001). Disturbances like flooding or fires can alter site trajectory and impact species composition (Middleton 1999). Landscape ecology and the spatial arrangement of a site influences

dispersal of organisms and connectivity to larger habitat blocks minimizes fragmentation (Bell et al. 1997). Guiding principles and theories of ecology apply to small-scale (e.g. bank stabilization plantings) and large-scale restoration projects (e.g. the Everglades and coastal Louisiana wetlands) (Simenstad et al. 2006). Wetland restoration ecologists must have cross disciplinary training to properly design and evaluate projects and there is never one straightforward approach; any methods or tools that can help practitioners streamline the process will greatly benefit the field.

Traditional methods for monitoring wetland restoration in coastal Louisiana are costly and labor intensive. They usually consist of vegetation plots, elevation surveys, areal extent estimates, and other measurements depending on the project's specific goals. Aerial photographs via airplanes might be taken every few years to analyze land and water changes. While these current protocols are the industry standard, rapid technological advancements may soon reduce the burden of collection. Technologies such as drones could replace the use of airboats and manned aircrafts in some circumstances. Drones provide significantly lower costs and improved human safety when compared to manned aircraft surveys, although the amount of areal coverage is greatly reduced (Christie et al. 2016). Because of the current costly methodology, many projects receive inadequate long-term monitoring.

Drones, or unmanned aircraft systems (UASs), offer a unique data stream that can help restoration practitioners understand the current state and potential future trajectory of a site. The technology has witnessed a rapid increase in ecological applications and a decrease in costs (Anderson & Gaston 2013; Klemas 2013; Pajares 2015). The resolution and variety of products that can be created from one drone survey hold powerful implications for short and long-term site assessments. Fine-scale site maps can help address gaps in monitoring and

provide a more ecological approach for essential principles like landscape context and position, comparison to natural habitats, and response to disturbance. UAS-derived maps provide managers a complete representation of the site with an accuracy of several centimeters. Although many studies have used remote sensing to assess restoration, few have capitalized on the use of drones specifically for monitoring and evaluation (Shuman & Ambrose 2003; Tuxen et al 2008; Klemas 2013; Knoth et al. 2013; Ridge & Johnston 2020). There is, however, a bottleneck of turning UAS data into meaningful products but advancements in software packages and analytic pipelines are continually progressing.

Processing methods for UAS datasets are frequently evolving (Woodget et al. 2017). Post-flight analysis is the most time-consuming aspect of drone work but advancements in methodologies are accelerating final product outputs. Structure from motion (SfM) photogrammetry and object-based image analysis (OBIA) allow for more in-depth information to be extracted from these records than with satellites or aerial photography. OBIA is a classification approach that has experienced a sharp increase in usage because of its capabilities to create accurate land cover and vegetation maps from high-resolution imagery (Blaschke 2009). The process consists of grouping similar pixels together into shapes using segmentation algorithms and assigning classifications based on spectral, textural, geometric, and contextual information (Laliberte & Rango 2009; Hossain & Chen 2019). Object-based methods utilize an interactive approach by letting the user build a set of rules that trains the software to identify objects based on certain criteria and essentially becomes a customized algorithm. The method has been used to conduct wetland plant classifications and map the spread of the invasive species like roseau cane (*Phragmites australis*) (Dronova 2015; Husson et al. 2016; Samiappan et al. 2016; Pande-Chhetri et al.

2017). These products can then be used to calculate landscape metrics like the aggregation index (AI) and assess fragmentation and habitat connectivity (McGarigal 2015).

Landscape metrics are useful for understanding restoration development and trajectory, however, it is not always straightforward what the results mean in terms of the ecology of a site (Kelly et al. 2011). Landscape ecology is based on the understanding of spatial arrangements within habitat mosaics and its influence on ecological phenomena (Turner 1989; Wiens et al. 1993). Advancements in sensors and software have led to an increased use of landscape metrics for assessing wetland configuration, fragmentation, and response to disturbance (Liu & Cameron 2001; Suir et al. 2013). Applying this type of study to wetland restoration benefits developmental analysis by informing local and regional habitat structure, providing guidance for selection of reference sites, and improving knowledge of wetland configuration and variation based on scale (Bell et al. 1997; Taddeo & Dronova 2019). Several studies have calculated landscape metrics from remote sensing data along the gulf coast and Louisiana (Suir et al. 2013; Couvillion et al. 2016; Stagg et al. 2019).

The Sabine National Wildlife Refuge (SNWR) is the largest coastal marsh refuge on the gulf coast. Located in southwestern Louisiana within the Calcasieu-Sabine Basin of the Chenier Plain, the refuge encompasses 50,586 ha (about 500 km²) of primarily wetlands. The area is essential for resident, migratory, and wintering bird populations as more than 200 species of birds can be spotted in the refuge. American alligators, river otters, and many other wildlife species rely on this region that straddles the two major water bodies in the area (Lake Sabine and Lake Calcasieu). Marshes deteriorated rapidly in the 20th century following

channel construction for mineral extracting and shipping purposes. The Chenier Plain region has lost approximately 900 km² of land from 1956 – 2006 (Barras 2008; Bernier et al. 2011).

Historically, the marshes were dominated by saw grass (*Cladium jamaicense*) and other intermediate to fresh species but shifted to more brackish water plants like saltmeadow cordgrass (*Spartina patens*) and saltmarsh bulrush (*Schoenoplectus robustus*) during the latter part of the 20th century (Miller 2014). Due to the persistent interior wetland loss, the area was chosen as a Coastal Wetlands Planning, Protection and Restoration Act (CWPPRA) project with construction beginning in 2001.

The SNWR Marsh Creation Project (CS-28) is a coastal wetland restoration plan that consisted of five separate dredge & fill cycles completed between 2002 and 2015. The goal was to create approximately 453 ha of new marsh habitat (Sharp 2011). Material was dredged from the Calcasieu Ship Channel by the Army Corps of Engineers to maintain navigation access and then pumped into containment areas to increase elevations and create new marsh. The primary objectives were to: (1) create new vegetated marsh and (2) enhance and protect existing surrounding marsh vegetation. Long-term monitoring consisted of three main criteria for which the sites would be evaluated: aerial photography for land and water analysis, vegetation plots, and elevation transect surveys. The area was chosen for this study because of the availability of pre-existing data and the proximity of sites to one another provided a unique opportunity for using drones to study neighboring restoration projects that range in maturity.

The goal of restoration is ultimately to restore wetland function but current methods for calculating success are inefficient and expensive. Drones are especially useful in places like the SNWR because sites are close together, results fulfill several aspects of monitoring

criteria, and methods are much less invasive than typical airboat surveys. Previous studies have used high-resolution datasets to monitor restoration progress but generally required manned aircraft flights or commercial satellites to achieve sub-meter pixel size which are both very high in price (Tuxen et al. 2008; Chapple & Dronova 2017). Stagg et al. (2019) used drone-based land and water maps, fragmentation/aggregation indices, and elevation surveys to determine flooding stress and hydrologic controls on healthy versus degrading marshes but few studies have looked at this in a restoration context. The detail of drone imagery has the potential to help managers translate success across sites and communicate results more effectively. My goal was to develop and apply methods for evaluating coastal wetland restoration using an off-the-shelf drone equipped with a regular RGB camera and integrate the results with traditional assessments.

Methods

Study sites. The study area is a mixture of natural and restored brackish marsh and shallow open water that experienced significant land loss due to canal building and altered hydrology, saltwater intrusion, and hurricanes (Louisiana Coastal Wetlands Conservation and Restoration Task Force 2012) (Figure 2.1). The Louisiana Coastal Protection and Restoration Authority (CPRA), U.S. Army Corps of Engineers, and U.S. Fish and Wildlife Service partnered to carry out restoration efforts. Construction practices for each project were generally consistent, but some variation in techniques allowed for comparisons of how different methods affected final outcomes. Dredged material from the shipping channel was pumped into containment dikes with the goal of a maximum initial elevation of 70 cm (NAVD88 Geoid 12A) and expected settlement to 9 cm after five years. Each site had a sediment “overflow” component where the containment dike was breached along the

lakeside levee to allow extra dredge material to flow out into open water and create additional marsh, but the technique only worked on one site (Cycle 2). Typically, tall stands of smooth cordgrass (*Spartina alterniflora*) expanded in the first few years taking each site about 3 – 4 years to become >70% vegetated (Miller 2014).

Project phases were completed from 2002 – 2015. Managers refer to the physical sites as cycles, so the term “cycle” is synonymous with site in this study. The timeline is as follows: Cycle 1 was finished in 2002, Cycle 3 in 2007 (note Cycle 3 was completed before Cycle 2), Cycle 2 in 2010, and Cycle 5 in 2015. Unfortunately, one site (Cycle 4) was excluded from this study due to complications with the imagery.

Cycle 1 had an original containment of 87 ha and was completed in February 2002. It is the oldest restoration site in this study (17 years). The site was pumped to an elevation of 55 – 67 cm (Sharp 2011), mean surface elevation was 14 cm after eight years (Miller 2014), and has been accreting at a rate of 0.4 cm/y since 2010 with the most recent average elevation reading at 22 cm (CPRA 2020). Cycle 1 was the only site planted and had trenasses (small man-made channels) manually dug during construction. Thirty-six thousand *S. alterniflora* sprouts were planted along the perimeter and trenasses. The site was 86% vegetated land after about eight years and 94% land after 14 years, surpassing its goal of creating 50 ha of marsh (Miller 2014; Beck et al. 2019). *S. alterniflora* was the dominant species until approximately seven years after construction when the community diversified to include seashore saltgrass (*Distichlis spicata*), saltmarsh bulrush, bulrush (*Schoenoplectus americanus*), and saltmeadow cordgrass. Monitoring was conducted by CPRA until a coastwide reference monitoring station (CRMS 6301) was established in 2009.

Cycle 3 was initially 93 ha and completed in May of 2007. It was pumped to an initial elevation of 12 – 61 cm. Pumping errors caused the site to be higher in the south and lower in the north with a wide range of surface elevations. Levees were breached every 150 m on the northwest side for the overflow technique, but it failed. Settled elevations were surveyed between -62 – 24 cm after six years with the majority of transects below targets, however, most transects were above the 9 cm goal after 11 years. The project area was 4.5% vegetated land after two years and 97.8% land after eight years (Miller et al. 2019; Beck et al. 2019). *S. alterniflora* was the dominant plant during early colonization, like Cycle 1, and Virginia glasswort (*Salicornia depressa*) established some stands initially but disappeared after a few years. Vegetation diversified eight years after construction with the emergence of *D. spicata*, *S. robustus*, and others but *S. alterniflora* remained dominant through 2018.

Cycle 2 had a containment area of 93 ha and was completed in May 2010. There is limited construction and historical monitoring data because it was converted to a state only project with no monitoring budget. The only available data is aerial imagery from 2015 and Suir et al. in revision satellite imagery. Unlike other sites, the “overflow” component was successful and created more than 40 additional ha of marsh outside the levees. This area will be referred to as Cycle 2 overflow (Figure 2.1). The site took longer to vegetate than other projects because unlike other sites, the levees were not breached until a few years after construction thus limiting tidal and hydrologic influence. Cycle 2 has been a *S. alterniflora* monoculture and it was 77% land in 2015 (Beck et al. 2019; Suir et al. in revision).

Cycle 5 was 94 ha and was finished in March 2015 with no initial elevation reported (Pontiff & White 2017). Three years after construction in 2018 the elevation settled to between -12 – 26 cm (Miller et al. 2019). Vegetation expanded rapidly post-construction and

the site was 64% vegetated land within 9 months. *S. alterniflora* was the dominant species with nominal percentages of other plants. The containment dike along the western edge has several major gaps, more than other sites, possibly resulting from erosion or initial construction practices (Pontiff & White 2017).

I used two nearby natural marshes as reference areas for comparisons. I chose them because they have been previously monitored by restoration agencies and are the largest stretches of marsh in the area. Reference North is a 50 ha marsh dominated by *Spartina patens* with swathes of *Spartina alterniflora* along its larger tidal sections and smaller amounts of *Schoenoplectus robustus*, *Schoenoplectus americanus*, and *Eleocharis spp.* across the site. Reference South is a 66 ha *Spartina patens* dominated marsh with pockets of water scattered across the interior of the site.

Planning and field work. All flights were conducted using a multi-rotor platform (Yuneec H520) due to vertical takeoff and landing capability. This hexacopter aircraft was designed for commercial use and chosen for my study because of high wind resistance, stability, and flight time (28 min). The H520 was equipped with an integrated autopilot system accessed through Yuneec's mission planning software (DataPilot). An important feature of the drone and software combination was the ability to seamlessly create, save, and load autonomous missions using satellite maps. The internal Global Positioning System (GPS) module geotagged images with an accuracy of 5 m horizontal and 8 m vertical. The hover accuracy of the aircraft was 1.5 m horizontal and 0.5 m vertical. The batteries are lithium polymer with an output power of 304 W and a capacity of 5250 Mah. Six drone batteries and a DuraCell deep cycle charging battery with a 12 V plug and terminal clamps were utilized to maximize survey coverage each day. On average, actual flight times ranged

from 15 – 23 minutes. The remote controller (Yuneec ST16S) was an Android-based all-inclusive transmitter with an 18 cm screen, joystick controls, and mapping and flight planning capabilities. The remote link transmission range is up to 1.6 km and video link resolution is HD 720p.

The sensor used to record images was a Yuneec E90 RGB camera. The dimensions are 115 x 80 x 130 mm and it weighs 350 g. Its 23 mm lens provides wide angle views with low distortion and increased sensitivity in low-light conditions and the diagonal field of view is 91°. The camera has a 2.5 cm CMOS sensor and its rolling shutter operates at 1/8000 – 4 s. Photo resolution was 3:2 (5472 x 3648) and effective pixels were 20 MP. The 3-axis gimble combined with the stability of the drone itself provided very stable camera positioning. The stability and gimble were important to avoid motion blur and create high-resolution orthomosaics from thousands of images, especially in windy coastal environments. Photo format is 10 – 12 MB JPEG files and the coordinate reference system was WGS84 UTM Zone 15N.

Flight plans were developed using Yuneec DataPilot desktop mission planning software. All flights were conducted at 68 m altitude above ground level using consecutive transects to cover the survey areas with an image overlap of 80% (frontlap and sidelap) and speed of 5 m/s. This altitude was chosen to maximize field of view while achieving < 2.5 cm GSD (ground sample distance) or pixel resolution in the final maps for a precise analysis of vegetation classes and to minimize possible blurred portions (Broussard et al. 2018). The angle of the transects was manipulated for each site to determine optimum battery efficiency. An east to west flight pattern was the most efficient for nearly all sites except Cycle 1 because its latitudinal distance put the aircraft out of range of the controller.

I installed ground control points (GCPs) around each site with one near approximate site center in addition to random checkpoints. GCPs are used to georeference the model and checkpoints are used to assess the final absolute accuracy. In general, six GCPs and three checkpoints were used at each site based on software manufacturer recommendations (Pix4D Mapper) and previous studies (Oniga et al. 2018; Manfreda et al. 2019). Coordinates were measured with a Trimble R10 GPS unit to ensure precise geolocation of GCPs and final products. Horizontal error of the GPS ranged from 1 – 15 cm and vertical error between 1 – 25 cm. The x , y , and z coordinates of 69 points were taken with an overall mean error of 1.2 cm horizontal and 2.1 cm vertical. In total, 46 targets were used as control points for georeferencing the imagery and 23 targets were reserved as horizontal and vertical checkpoints to help assess accuracy of the data. Point data were compiled into .CSV files at each site for processing within the Pix4D photogrammetry software.

Drone flights were conducted in the summer of 2019 from late June – mid-July between approximately 9:30am – 1:30pm Central Daylight Time (equipment malfunctions caused delays in some cases). All flights were conducted from a watercraft (6.5 m SeaArk bay boat) with a 1.5 x 1.2 m front deck area for landing and takeoff due to site conditions. Surveys were mostly automated, but I determined when to recall the drone at low battery and manually landed on the bow. On average, five batteries were used at each site. Seven sites were surveyed over a three-week period (June 26 – July 18) but only six were used in this study. In total, 37 flights were conducted.

Field surveys were conducted to verify the remotely sensed data and compare the sites using traditional monitoring methods (Figure 2.2). Nine total 2 x 2 m quadrats were surveyed at each site for species composition, plant height, and percent cover of vegetated

and unvegetated surface. The methodology was chosen based on the Braun-Blanquet cover scale used by the USGS Coastwide Reference Monitoring System (CRMS) and CPRA protocols that have been used to monitor these sites in the past (Folse et al. 2014; Miller 2014). Most cycles are bounded by remnant containment dikes from restoration that form the edges of the site, however, in some cases marshes have expanded outside them and additional plots were measured along these transects to capture the edge and dike plant communities. A full list of species is included in Table 2.1.

Processing and analysis. The flight images were mosaicked within the software Pix4D Mapper (version 4.4.12) to create orthomosaics and 3D digital surface models (DSMs) using structure from motion (SfM) algorithms. Orthomosaics are detailed and georeferenced photo representations of the area, essentially high-resolution maps, constructed from multiple images (several thousand per site in our case) and DSMs are representations of the surface and the tallest objects like vegetation or structures, like a digital elevation model (Figure 2.3). The SfM technique has revolutionized analyzing surface structure in ecology and is perhaps the most practical and affordable alternative to LiDAR (Forsmo et al. 2019). Algorithms use overlapping, geotagged 2-dimensional images to model the surface of an area and recreate it into a 3-dimensional model. The geolocation details and image overlap allows software to match images and reconstruct the scene.

Once images were uploaded, the software detected camera parameters, image coordinate system, and altitude and location details for each picture. The coordinate system output for the orthomosaics was WGS84 UTM zone 15N. I used the 3D maps processing template in Pix4D to create an orthomosaic, point cloud, and DSM. GCP and checkpoint measurements were uploaded with x , y , and z coordinates and horizontal and vertical

precision error values and the targets were verified using the ray cloud editor. Manual tie points (MTPs) were also added in the ray cloud to improve reconstruction accuracy and clarity in the final orthomosaic. MTPs are points created after initial processing by marking or clicking the exact same point at a site in multiple images. Processing was conducted on a Dell Precision Tower 5810 desktop with 32 GB of RAM (random-access memory), an Intel Xeon CPU E5-1603 v3 @ 2.80GHz, and a NVIDIA Quadro M2000 GPU. Processing times ranged from 18 – 48 hours per site. A total of 20,515 raw images were processed to create 686 ha of mapped area with an average pixel size of 2.2 cm (excluding Cycle 4).

Two products were created by combining the orthomosaics and DSMs: (1) land and water maps and (2) vegetation species/dominant group classifications (Figure 2.3). Classes were assigned based on the ground reference data. Land and water classes were delineated based on rules developed by Cowardin et al. (1979) where land was considered all vegetation including marsh, scrub/shrub, emergent vegetation, and exposed bare ground on the containment dikes (which is higher elevation and does not flood). Water was considered open water, nonvegetated mud flats, floating aquatics, and submerged aquatic vegetation.

The restoration sites all contained the following six classes: bare ground, *D. spicata/S. patens*, *Phragmites australis*, *Spartina alterniflora*, scrub shrub, and water. Bare ground was considered exposed, unvegetated bare soil on containment dikes. The *D. spicata/S. patens* class represented vegetation stands where *Distichlis spicata* or *Spartina patens* were the dominant species. These two vegetation types were difficult to distinguish at the restored sites so the species were grouped, although *D. spicata* was more common based on field surveys. Often these stands were mixed with smaller percentages of *Schoenoplectus robustus* or *Schoenoplectus americanus* with nominal percentages of other species. The

Phragmites australis class represents roseau cane or common reed which is a grass that forms dense stands reaching heights of 1 – 6 m. From here on, it will also be referred to as *Phragmites*. *Spartina alterniflora* represents vegetation stands where smooth cordgrass was the dominant species. *S. alterniflora* was sometimes mixed with *S. robustus* and other species. Scrub shrub primarily consisted of Jesuit's bark (*Iva frutescens*). The reference sites contained similar classes, but both had a *Spartina patens* category because it is the dominant species at both sites. Reference North also had an *Eleocharis spp.* class because it contained a few dense stands of the vegetation.

An object-based image analysis approach was used to conduct vegetation mapping with the software eCognition Developer (Figure 2.4) (v. 9.5, Trimble Germany GmbH, Munich, Germany). Orthomosaics and digital surface models (DSMs) provided four layers to use in image analysis (Red, Green, Blue, & DSM). Individual “rulesets” were developed for each site using similar approaches and parameters to assign classes to cover types. Rulesets are a step by step process of segmentation (grouping pixels into meaningful shapes e.g. water bodies or trees) to create objects and classification of those objects based on attributes or “features”. Cycles 3 and 5 and Reference South were completely automated using ruleset development which included a supervised classification as the last step to separate grass species (after other classes had been identified using threshold values of various features) and no manual editing was performed. The other three sites were initially classified into grass, *Phragmites*, bare ground, and water using basic rules and manual editing. From these initial classifications water, *Phragmites*, and bare ground were preserved, and the grass class was segmented and classified following methods for the other sites. Although the techniques

varied slightly, comparisons across sites were valid because spatial resolutions are identical (~2.2 cm GSD) and overall accuracies were similar.

The three automated sites (Cycle 3, Cycle 5, and Reference South) were analyzed by running segmentation algorithms for each class of interest. Segmentation is a key step because its outcomes have a significant impact on accuracy (Dronova 2015). It was a subjective process of trial and error to find the right combination of scale, color/shape, and compactness/smoothness within the “Multiresolution Segmentation” algorithm which is a common problem in OBIA (Baatz & Shaape 2000). All sites began with the classification of water. A multiresolution algorithm using scale parameter of 30, shape 0.3, and compactness 0.75 (with only red, green, and blue layers) followed by a spectral difference segmentation using a scale of 5 (using all layers, including DSM) yielded the best results for separating water from vegetated marsh. The addition of the spectral difference algorithm helped increase the object size for larger water bodies, making classification easier with fewer objects, while still capturing small pockets and channels that were important for fine scale analysis. The texture feature grey-level co-occurrence matrix (GLCM) homogeneity: all directions and the spectral features normalized difference index (NDI) Green – Blue and mean brightness were the most useful for initially classifying water (Laliberte & Rango 2011; Husson et al. 2016). The normalized difference index is calculated using the mean values of the two bands (Hunt et al. 2005).

$$NDI = \frac{Green - Blue}{Green + Blue}$$

NDI values for other band combinations were used to identify vegetation later in the process. Bare ground was occasionally misclassified as water but could typically be separated using high mean brightness values, sometimes texture, and distance to scene border

because the only bare ground was along the containment dikes. Remaining unclassified objects were merged and segmented for the next class. *Phragmites* was next because it could typically be identified using the mean DSM values. *Phragmites* was generally much taller than surrounding plants in these marshes. Objects with a mean DSM value of greater than or equal to 1-2 meters were usually assigned to the *Phragmites* class. A multiresolution algorithm with a scale parameter of between 100 - 150, shape 0.3, and compactness 0.75 produced the best results for segmenting *Phragmites*. One major issue with the use of DSM values was that several of the sites had flaws in the surface models (Figure 2.3b). This was overcome by using x and y distance to scene borders for target areas. It is possible that smoothing or resampling the surface models to a lower resolution would help overcome this issue, but our method was quick and effective for reducing misclassifications. Rules used to refine initial classifications for *Phragmites* included relative border to *Phragmites*, a mean DSM value of around 1.5 meters, and mean brightness. Scrub shrub was next, and in some cases, the same segmentation for *Phragmites* was used. Otherwise objects were merged and segmented with another multiresolution algorithm using scale parameter of 50, shape 0.3, and compactness 0.75. Objects with a mean DSM greater than 1 meter were initially classified as scrub shrub and refining rules utilized the mean difference to neighbors DSM and textural features. Lastly, a spectral difference algorithm with a maximum spectral difference of 3 - 10 was applied to segment and enlarge remaining unclassified objects. The last 2 classes analyzed were *Spartina alterniflora* and *D. spicata/S. patens* (*Spartina patens* and other for Reference South). Training samples of each were selected and a Nearest Neighbor supervised classification was run using the four features: NDI Green – Red, brightness, mean DSM, and area.

The first three sites that were analyzed (Cycle 1, Cycle 2, and Reference North) were done using one round of segmentation, basic rules to separate bare ground, marsh vegetation, water, and *Phragmites*, and additional manual editing. The parameters for the multiresolution segmentation were scale 150, shape 0.3, and compactness 0.75. Initial features used to define classes were mean brightness, mean red band, mean DSM, roundness, area, and position values for individual objects. Misclassified areas were identified through careful visual inspection and photo interpretation of the orthomosaic and classified layer then reclassified through additional thresholding of other parameters or manually edited into the appropriate cover type. Water, bare ground, and *Phragmites* classes were retained for these sites and the remaining vegetation was classified using the same methods for the automated sites.

I exported classifications as vector layers with area (m²) and border length (m) included as attributes. Accuracy assessments consisted of approximately 500 stratified random sampling points per site using ArcMap (10.4.1). I created an error matrix for each site using orthomosaics as reference datasets for determining classification accuracy (Congalton 1991). All border length and area statistics were aggregated and analyzed in ‘R’ (v 3.5.1, R Development Core Team).

Landscape metrics, otherwise known as spatial pattern metrics, quantify aspects of a habitat’s organization and structure and are commonly calculated using GIS data products. Class areas, percentage of landscape, number of patches, patch density, edge density, and aggregation index (AI) were calculated based on usage in previous studies (Broussard et al. 2018). I used land and water classes for these metrics because I was interested in water body configuration and general, as opposed to class specific, vegetation dynamics. Image resolutions were resized to 5 cm resolution for calculations. Patch is a widely used term in

landscape ecology and was defined here as a habitat unit that differed from its surroundings based on the resolution of the files (e.g. a piece of land isolated by water). The ecological meaning of all spatial pattern metrics is scale dependent and in general, results are most relevant to a question or an organism. Meaning that I calculated these metrics at a high resolution to achieve the highest accuracy, but most humans or wildlife would not consider a 5 x 5 cm patch of land an island. However, results can be recalculated using a larger scale to fit a research question or track an ecological process like fragmentation. For example, managers interested in a particular nesting bird with knowledge of its habitat size preferences can rescale the data to fit that species' perspective of the environment.

Aggregation index (AI) is a widely used metric for evaluating landscape structure and is the frequency with which patch types appear side by side and quantifies the tendency of a patch to appear in large, grouped distributions (He et al. 2000; McGarigal 2015; Couvillion et al. 2016). An example of two different pieces of marsh with corresponding AI values is shown in Figure 2.5. Number of patches is an indicator of the fragmentation of a class based on the total number of isolated patches present on the landscape. Patch density is the number of patches per unit area based on total landscape area in square meters. Edge habitat in this study was considered the marsh to water border. Since the sites were cropped to the marsh edge and no water was classified outside the boundaries, the border length of the water class was used as a proxy for interior edge habitat. Exterior edge habitat was then the total length of the land class minus the amount of interior. Portions where continuous habitat was cut off due to flight coverage were measured and subtracted from total edge calculations. Edge density was also calculated which is the amount of edge per unit area, standardized for

comparisons across areas of different sizes. All landscape configuration metrics were calculated in ‘R’ using the Landscapemetrics package (Hesselbarth et al. 2019).

Floristic Quality Index (FQI) provides an estimate of wetland quality based on species composition and percent cover of a plant community (Gianopoulos 2014). FQI is scored from 0 – 100 (following CRMS protocol) by combining coefficient of conservatism (CC) values assigned to specific plants by a panel of coastal vegetation experts and field-based percent cover estimates. A high value means the site contains ideal species compositions for the region based on plant rankings and native species and a low value indicates less than ideal habitat likely containing invasive and disturbance prone species. Coefficient of conservatism values are regional or state specific and plants are also assigned to general classes: invasive species (CC = 0), disturbance species (CC = 1-3), less vigorous communities (CC = 4-6), common vigorous communities (CC = 7-8), and dominant species (CC = 9-10) (Suir & Sasser 2017). Scores used in this study were based on ones used in Suir et al. in revision. Modified Floristic Quality Index (FQI_{mod}) was calculated using field survey data to compare to CRMS and Coastal Wetlands Planning, Protection and Restoration Act (CWPPRA) metrics using the formula:

$$FQI_{mod\ t} = \left(\frac{\sum (COVER_{it} \times CC_i)}{100} \right) \times 10,$$

where COVER_{it} is the percent cover for particular species *I* at a sample unit in a sample site at time *t* and CC_{*i*} is the coefficient of conservatism value for species *I* (Cretini et al. 2011). The index has been shown to be useful for assessing wetland restoration maturation and detect plant community changes over time (Lopez & Fennessy 2002).

I compared my overall field and drone-based results with previous analysis of the sites conducted by monitoring agencies and Suir et al. in revision. Field monitoring data were

compared to information from CPRA surveys in 2018, CRMS data from 2018, and Suir et al. in revision data from 2015 that consisted of species composition, percent cover, and FQI calculations. CRMS is a statewide network of stations to provide data for restoration decision making. UAS data was compared to land water classifications of 1 m resolution aerial imagery (USGS) acquired in late 2015 and 0.31 – 1.2 m resolution WorldView-3 imagery (Suir et al. in revision) acquired in early 2016. UAS classifications of the restoration sites were masked to same extent as the satellite data using shapefiles from the previous study.

Results

The restoration sites were between 73 – 96% land based on summer 2019 drone-based land and water classifications (Table 2.2; Figure 2.6). The youngest restoration site (Cycle 5) was the lowest at 73.2% land and the oldest site (Cycle 1) had the highest coverage at 95.5% land (Figure 2.7). The two middle aged sites (Cycles 2 & 3) were even at 86.5% and 86.4% land, respectively. The land and water analysis revealed that the marsh creation sites exhibited rapid expansion of vegetated land in the first four years post-construction (18 %/y) and then gradually for the next 10 – 12 years (2.4 %/y) until sites surpassed proportions of reference marshes. These findings support previous remote sensing analysis of the restoration sites in regard to percentages and rates of expansion over time (Miller 2014; Beck et al. 2019; Suir et al. in revision). Cycle 2 created the most marsh out of all sites by 48 ha due to the success of the overflow technique. Cycle 2 was 86.5% land including the overflow area and 84.6% excluding the overflow (only inside the original containment dikes). The reference sites (North & South) were also close in configuration at 91% and 92% land, respectively (Figure 2.7).

The younger restoration sites were dominated by *Spartina alterniflora* while the older sites showed a pattern of more mixed vegetation types with higher amounts of *D. spicata*/*S. patens* (Figure 2.8). In general, the restored sites exhibited rapid invasion of *Spartina alterniflora* in the first 10 years followed by an expansion of *Distichlis spicata*, *Spartina patens*, and *Schoenoplectus robustus* with small percentages of other species. Figure 2.9 shows the breakdown of percent cover values across sites. The two younger sites, Cycle 5 (Figure 2.10) & Cycle 2 (Figure 2.11), were 64% and 76% *Spartina alterniflora*. The two older sites, Cycle 3 (Figure 2.12) & Cycle 1 (Figure 2.13), were 36% and 31% *Spartina alterniflora*. In contrast, the reference sites were dominated by *Spartina patens*; North was 67% and South was 78% *S. patens*. Reference North had 14% *Spartina alterniflora* cover and Reference South did not have any (Table 2.7). Overall accuracies for the classifications were between 75 - 90% with a mean overall accuracy of 83%. Kappa values ranged 0.54 – 0.82 with an overall mean of 0.68 (Tables 2.8 – 2.13). Kappa ranges from 0 – 1 with 0 indicating no agreement between the reference image and classified image and 1 indicating the highest level of agreement. I achieved the highest accuracy, 90% overall, at the two youngest restoration sites probably because they had less diverse vegetation communities (Tables 2.8 & 2.9). The least accurate classification was 75% at Cycle 1 which had the highest average species richness (Table 2.10, Figure 2.13).

The field survey-based species assemblage of the restoration sites reflected the drone-based dominant species classifications (Figure 2.15). Cycle 3 had a higher amount of *S. patens* than any other restoration area but this could be due to sampling location bias as a result of site accessibility. Previous studies found a higher percentage of *D. spicata* (Miller 2014). Figure 2.16 shows a trend of increasing diversity and percent vegetated cover over

time with Cycle 1 containing a higher number of species on average than the reference locations. Cycle 2 created by far the most marsh but had the lowest species richness with one species per site on average (Figure 2.16). The group means are significantly different from one another for species richness (ANOVA, $F_{5,49} = 2.01$, $P = .0941$) and percent cover (ANOVA, $F_{5,49} = 6.28$, $P = .0001$) (Figure 2.16). The older restoration sites, Cycles 1 & 3, had Floristic Quality Index (FQI) scores close to that of Reference South; all between 71 and 74 (Figure 2.17). The CRMS monitoring site for Cycle 1 calculated a score of 78 for 2019. Reference North had the highest FQI score of 85 and Cycle 2 had the lowest at 56. FQI is an index of wetland habitat quality based on scores assigned to plants thus ranking their value to the region. The reference sites had an average score of 79 which is close to the ideal score of 80 for Chenier Plain brackish marsh (Cretini et al. 2011). The results of the restored sites indicate the marshes approach this ideal range after about 12 years.

Comparisons to previous remote sensing data show the land and water interface calculations were the closest across sensors and years for the most mature restoration site, Cycle 1 (94 - 96% land) (Table 2.3). Prior to drone flights in 2019, the most recent remote sensing surveys of the area used 1 m resolution aerial imagery and 0.31 – 1.24 m satellite imagery from late 2015 and early 2016, respectively. The largest differences occurred with the youngest site, Cycle 5. There was a 35% difference in the amount of land between satellite (29%) and aerial photo (64%) calculations but this was likely caused by classification methods. Cycle 5 was 73% land by 2019 based on drone data (Table 2.3). The 2019 drone assessments displayed higher percent land values than previous assessments for all sites except Cycle 3. Estimates decreased from 94 – 98% land in 2015/16 to 86% land in 2019 (Table 2.3).

The dominant species group was the same across sampling techniques at all sites except Cycle 3 (Figure 2.18). Agency field surveys from 2018 (both CRMS and CPRA) estimated *Spartina alterniflora* was the dominant cover type but 2019 drone classifications and personal field surveys estimated *Distichlis spicata/Spartina patens* was the dominant group. Overall, previous vegetation data collected by restoration monitoring agencies and field survey data collected at the same time as the drone flights support the assertion that as sites mature, low marsh *Spartina alterniflora* cover declines in these brackish marshes while high marsh *Distichlis spicata/Spartina patens* and other vegetation types expand (Figure 2.18) (Miller 2014; Suir et al. in revision). Figure 2.18, however, highlights differences in results across sampling methods.

Cycle 2 had the highest amount of interior and exterior edge habitat, it was the largest site, but it had the most interior edge by 40 km due to success of the overflow technique (Table 2.4, Figure 2.11). Edge habitat was considered the marsh/water border in this study. Cycle 3 had the highest interior to exterior ratio of 7.9 calculated by dividing the amount of interior by the amount of exterior edge in kilometers (Table 2.4). The youngest sites had the three highest ratios and the oldest restoration site and references had the lowest ratios of 3 - 4. Edge is a commonly used metric in landscape ecology and is an important driver of consumer biomass in saltmarshes (Minello et al. 1994). The high aggregation index values for our study sites indicate that land and water are very connected to one another and comprise a landscape characterized by low fragmentation (Table 2.5). Although the sites are characterized by mostly “intact” stands of connected marsh, these high AI values were surprising. Cycle 2 area within the original containment dikes had an AI score of 99.7 for water and the overflow analyzed separately had a score of 97.4 for water, making it the

lowest AI score out of all sites. The reference sites and oldest restoration site (Cycle 1) all have a low AI value of 98.8 for the water class meaning water bodies are more scattered across those sites. Cycle 1 had the lowest patch density for land (168 patches/100 ha) and water (435 patches/100 ha) classes indicating it was a more spatially connected site with less scattered patches of habitat even though the AI value for water (98.8) was slightly less than other restoration sites (99.1 – 99.7). Although Cycle 3 had the highest interior to exterior edge ratio (7.9), Cycle 2 had the highest edge density (954 m/ha) which is more representative of the number of small channels present on the landscape (Tables 2.4 & 2.5; Figure 2.11). Cycle 1 had the lowest edge density (423) (Table 2.5; Figure 2.13).

Discussion

My results demonstrate the use of an off-the-shelf drone as a tool to help understand the ecological sequence of restoration and ultimately project success. The high-resolution maps provide a more holistic perspective of sites than traditional surveys. Using these products, I quantified how much land was created, how plant community structure shifts as sites mature (using a space for time substitution), and how the hydrology and spatial arrangement of channel networks function as a result of construction practices thereby informing marsh development. However, determining the highest level of success is not entirely straightforward.

Understanding success for a constructed wetland project is difficult due to a lack of standardized methods and because of uncertainty regarding when or if functional attributes of restored habitats should mimic those of natural systems (Morgan & Short 2002). All four restoration projects were successful in achieving the >70% land target based on manager goals. Classification results also confirm agency reports that dominant species compositions

shift over time from low marsh (*S. alterniflora*) to high marsh plants (*D. spicata*/*S. patens*) (Miller 2014). But none of the restored site communities mimic those of reference areas. And there are potential tradeoffs to structural configurations and biological characteristics, like less edge habitat but higher species richness with age. It should be noted that restoration results and community structure findings from these southwest Louisiana brackish marshes were driven by site specific factors like salinity, tidal range, dredge sediment composition, and other variables and development may differ in other regions. It is hard to draw absolute conclusions due to timeline and construction differences, but sites with more edge habitat and interior water in our study had more *S. alterniflora*. Although a possible function of time in this case, tidal influence does dictate zonation of herbaceous vegetation and *S. alterniflora* is generally more flood tolerant than *S. patens* (Broome et al. 2019; Bertness 1991).

The expansion of high marsh species at restored sites can be partially explained by elevation accretion. In tidal settings, the range and relative marsh elevation is very important in controlling the frequency, duration, and depth of inundation which in turn influences community structure (Mitsch & Gosselink 2015). Cycle 1 has been accreting at a rate of 0.36 cm/y since 2009 and shifted from a low marsh to a high marsh dominated site after approximately 10 years even though managers planted it with *Spartina alterniflora* (Miller 2014; CPRA 2020). Cycle 3 was naturally colonized by low marsh during initial development but elevations increased from 2013 to 2018 and based on transect surveys, the site was higher in the southern end which coincided with drone-based classifications of high marsh species occurrence (Miller et al. 2019). The only major section of high marsh in Cycle 5 was in the northern portion and the highest elevation transects were also in the site's northern half based on 2018 survey results (Miller et al. 2019). Although most of the high

marsh habitat at the restored sites was *D. spicata* and the natural marshes were predominately *S. patens*, the community shift is a positive indicator for restoration development and elevation accretion.

Vertical accretion in marshes comes from two main sources, flooding accompanied by sediment deposition and organic material accumulation from plant biomass (Morgan & Short 2002). The physical setting and hydrologic influence have a major effect on which species occupy certain spaces but the plants themselves also influence sediment trapping rates and organic matter buildup through stem densities and aboveground vs. belowground biomass. Together, these ecological interactions facilitate marsh development, vegetation survival, and future stability (Morris et al. 2002; Kirwan et al. 2016). Constructed marshes can attain similar aboveground production values to reference sites within the first few years, but soil organic matter may take decades (Craft et al. 1999; Suir et al. 2019). Elevation and frequency of inundation also impact aboveground biomass and soil organic matter with species specific effects (Craft et al. 2002). For example, in a brackish constructed North Carolina marsh, *S. alterniflora* developed similar biomass levels to natural marshes within three years but *S. patens* planted at higher elevations did not within 15 years (Craft et al. 2002). At my sites, *D. spicata* was the primary high marsh species to expand with the increases in elevation and it will be interesting to see if this was a function of initial colonization that will be followed by more competitive interactions with the dominant reference species *S. patens*. Managers, in this case, were primarily concerned with creating vegetated marsh and not so much species compositions or ecological characteristics like soil organic matter. Drone surveys do not directly examine any functional attributes but do

provide excellent structural representations of sites with which future studies could pair these variables.

Spatial pattern metrics indicate variable results for vegetation expansion and overall site configuration. Cycle 1 had the lowest number of patches, patch density, and edge density which means it was the most continuous and uniform marsh site in the study. It had the highest land percentage (96%) and most of the water within the site was connected by the man-made channels. Out of all the metrics, edge density was the most representative of site arrangement because it accurately portrayed the amount of interior water at each site and showed that Cycles 2 and 3 had more similar layouts to the reference marshes. Previous studies resampled resolutions to calculate landscape metrics and I think finding the appropriate thresholds and scale of interest would have made the patch results more meaningful in my study (Stagg et al. 2019). Although scaling metrics for a particular question or organism can provide greater ecological information, these measures may be more useful for tracking site changes over time (Kelly et al. 2011).

Drone-based estimates for amount of vegetated land aligned with other remote sensing calculations for the oldest restoration site, but other sites had significant differences. Most notably, Cycle 3 was the only restored site that showed a decline in the amount of marsh (98% in 2015 to 86% 2019). The northern portion of the cell was shallow open water for the first five to seven years while the rest of the site vegetated because of improper pumping (Miller et al. 2019). The entire site had vegetated by 2015 even though 2018 elevation transects in the northern end were still below target goals (Beck et al. 2019; Miller et al. 2019). Drone imagery from 2019 showed the same area had returned to open water (Figure 2.12). Water surface elevation readings from the CRMS 6301 hydrologic station

revealed an 11 cm difference (NAVD88 Geoid 12A) for the two dates of imagery capture at 26 cm (7 December 2015) and 37 cm (28 June 2019) (CPRA 2020). Perhaps flooding bias on imagery acquisition dates and variations in calculation methods or data resolution caused the difference, however, it is possible the low elevations and large tidal channel could have facilitated a loss of vegetation and return to open water.

Successes and shortcomings of construction practices were also highlighted by the resolution of drone imagery. Cycle 2 was the only site where the overflow technique was successful thus creating 45 ha of additional marsh but has little monitoring data (Figure 2.14). Managers have attempted a similar approach at another location in the refuge by placing dredge material in a shoreline cove rather than use containment dikes (CS-81) (Louisiana Coastal Wetlands Conservation and Restoration Task Force 2018). Cycle 2 was the second youngest site (9 years old) but contained the most land by 30 ha, was within 5% of the reference marsh percent land values, and had the highest amount of interior edge by 40 km (Tables 2.2 & 2.3). Although plant species diversity was the lowest, the site may be the most beneficial to aquatic organisms. Novel methods used to interpret energy production for white shrimp based on habitat cover demonstrated the importance of edge habitat in these areas as a driver for consumer biomass and abundance (Nelson et al. *in review*). Edge in coastal marshes can also support higher bird species richness than other habitat types (Patton et al. 2020). Cycle 2 was the most successful project based on manager goals for land creation and perhaps species diversity will develop as the site matures.

My primary objective was to develop a method using object-based image analysis to classify dominant marsh species (Figure 2.20) and develop a workflow that others can build upon to assess future restoration efforts. Further analysis to refine classification techniques

would improve results and likely lead to more in-depth species maps. I used RGB orthomosaics and elevation information from digital surface models to identify water, bare ground, *Phragmites australis*, and shrubs using threshold values and then applied a supervised nearest neighbor classification for the remaining vegetation using training samples. Methods were based on previous studies of wetlands and the general framework should apply to similar habitats but certain differences between my rulesets highlights the subjectivity of site-specific object-based classification approaches (Laliberte & Rango 2009; Dronova 2015; Husson et al 2016; Pande-Chhetri et al. 2017; Broussard et al 2018). For example, the spectral difference segmentation algorithm scale had to be reduced at one site because it grouped a large section of two different plant species together. This reduction made the object sizes smaller leading to an increased processing time of six to almost 24 hours for the nearest neighbor classifier. Smaller objects also led to more misclassifications at some sites. For example, figure 2.13 shows the somewhat patchy classification results for Cycle 1 which possibly could have been improved with a higher scale.

Object-based image analysis is a powerful technique and has many advantages over pixel-based approaches, but ruleset and feature selection can vary widely depending on the user, type of imagery, time of day, and many other factors. The DSM information was also critical in this study, especially for classifying *Phragmites*, however, some portions of the models were flawed and open water can create extreme high and low elevation values with drone imagery. I worked around these issues by targeting specific sections of each site when using height data to identify *Phragmites*. The issue may have been a product of our aircraft's internal GPS vertical accuracy and perhaps the addition of more ground control points, especially around stands of *Phragmites*, would have improved our models.

I demonstrated the use of an off-the-shelf multi-rotor aircraft for relatively large 90+ ha ($\sim 1 \text{ km}^2$) site surveys from a boat. Although fixed-wing aircrafts are more suited for larger areas, wetlands may not have favorable landing ground; therefore, multi-rotor platforms are better suited for some marsh situations. Price ranges widely for drones but most quality multi-rotor aircrafts are significantly cheaper than similar quality fixed-wing models. There is also a lower barrier to entry with multi-rotor aircrafts for those interested in integrating drones into their research and my goal here was to demonstrate the accessibility of drones as a research tool. The ease of piloting, ability to hover, and improvements in flight planning software and automation make multi-rotors available to anyone willing to put in the training for coastal surveys.

Advanced sensors, for example multispectral cameras that can capture near-infrared and rededge bands, have been widely used for vegetation studies and benefit analysis of wetland plant health through indices like the normalized difference vegetation index, but these are not always available to researchers (Boon & Tesfamichael 2017; Diaz-Delgado et al. 2019). Most multi-rotor drones come equipped with an integrated high-resolution RGB camera that, paired with modern SfM processing techniques, can generate powerful datasets for logistically difficult areas. The purpose of scientific study, primary research questions, and user experience should drive overall equipment choices. Multispectral data is hugely beneficial in more complex wetland environments where additional spectral information helps delineate species when 10 or maybe 20 types of plants are mixed; and it is necessary for vegetation health and stress analysis. But my research helps demonstrate the utility of regular RGB imagery for classifying dominant species and these techniques may be more appealing to small scale wetland scientists than the use of precision sensors. For example,

mitigation banks could easily incorporate an off-the-shelf drone into surveys so that wetlands are quickly inventoried and reported to permitting agencies without using specialized hardware and equipment.

By combining remote sensing and field surveys, I was able to better understand restoration success through accurate water and vegetation mapping, land creation analysis, and spatial arrangement metrics. All sites reached manager goals of 70% land composition but the sediment overflow technique made Cycle 2 the most successful. Restored wetlands displayed a general trend of increasing species diversity with age and a shift in dominant species after about 10 years. *Spartina alterniflora* dominated younger sites and was more common in flooded areas with more edge habitat at all sites. Although vegetation communities do not mimic those of reference marshes, spatial metrics and fragmentation indices indicate that restoration sites become equally or more aggregated than natural marshes after approximately 12-15 years. Drone imagery also revealed subtle differences in site development that were not captured by previous monitoring data. For example, the expansion of high marsh species *D. spicata* and *S. patens* in the northern portion of Cycle 5 after just four years (Figure 2.10).

High-resolution drone imagery helps us understand ecosystem development because of the holistic site level data it provides. Field surveys are essential to determine species composition, but that same data can be used to create realistic habitat configurations by pairing it with drone surveys and training software instead of extrapolating from plot transects. The detail of the imagery gave me the ability to delineate dominant marsh species across sites and investigate how plant configurations were structured in relation to fine-scale water bodies and channels. I also accurately mapped the invasive species *Phragmites*

australis which was underrepresented in previous field surveys. *Phragmites* can help marshes persist by trapping sediment with its dense cane stands, but major die-offs have occurred in coastal LA because of an invasive scale insect from Asia and other reasons that have led to a significant increase in research. Samiappan et al. 2016 also demonstrated the utility of drones for mapping *Phragmites*. In general, processing methods were time consuming, but continual refinement will speed up the workflow and techniques could be improved and standardized for this region. The imagery also serves as a baseline for future research, because although previous remote sensing studies have been conducted at the sites, the resolution of the drone imagery is significantly higher than any other source.

Future studies using drones to survey marshes should consider a few changes to my approach. Project objectives and questions generally determine methodological parameters and there are tradeoffs to different approaches. For example, I would fly at a slightly higher altitude to reduce the number of images and speed up processing time, but you obviously lose resolution. I chose 68 m because our software calculated I would achieve a 2.2 cm pixel resolution on the ground; next time, I would aim for 2.5 cm or slightly higher. I would also fly earlier in the morning to make the classification of water easier. Lower wind and sun glare make the use of textural and spectral features more effective for using RGB imagery but can lead to more shadows if taller objects are present on the landscape. OBIA segmentation scale parameters and the combination of multiresolution and spectral difference algorithms worked very well for delineating water across sites, but scales were not as consistent for delineating marsh grasses. The maximum spectral difference scale of 10 worked for some sites, but it had to be reduced for others so that different species were not grouped together. Unfortunately, this reduction led to a higher number of smaller objects and

more misclassifications. To speed up processing time, after classifying water, I would merge and segment remaining objects at a scale of 125 and eliminate a separate segmentation for shrubs. I would use DSM values and other features to identify *Phragmites* and then incorporate the scrub shrub class into the supervised nearest neighbor classification. Studies could also incorporate wildlife observations captured in drone imagery to add faunal components for more holistic observations.

Drones have revolutionized spatial ecology and the technology's use has rapidly increased across many scientific disciplines because its operational flexibility, high-quality/low-cost data, and repeatability (Anderson & Gaston 2013). The current regulatory environment managed by the FAA and user-friendly flight planning software makes using drones a viable option for any researcher. No other remote sensing method offers such high detail for the price. The biggest caveat is processing time but methodological refinement and advancements in computing and software packages will continually reduce the time burden. Coastal research would significantly benefit from increased use of the technology and further efforts to improve automated processing techniques.

Tables

Table 2.1 Plant species surveyed in restored and reference sites at the refuge

Scientific Name	Common Name
<i>Spartina alterniflora</i>	smooth cordgrass
<i>Spartina patens</i>	saltmeadow cordgrass
<i>Schoenoplectus robustus</i>	saltmarsh bulrush
<i>Distichlis spicata</i>	seashore saltgrass
<i>Paspalum vaginatum</i>	seashore paspalum
<i>Borrchia frutescens</i>	bushy seaside tansy
<i>Iva frutescens</i>	Jesuit's bark
<i>Amaranthus australis</i>	southern amaranth
<i>Ipomoea sagittata</i>	saltmarsh morning glory
<i>Schoenoplectus americanus</i>	chairmaker's bulrush
<i>Baccharis halimifolia</i>	eastern baccharis
<i>Symphyotrichum tenuifolium</i>	perennial saltmarsh aster
<i>Eleocharis spp.</i>	spikerush or spikesedge
<i>Vigna luteola</i>	hairypod cowpea
<i>Cladium mariscus</i>	Jamaica swamp sawgrass
<i>Setaria magna</i>	giant bristlegrass
<i>Salicornia depressa</i>	Virginia glasswort
<i>Cyperus odoratus</i>	rusty flatsedge

Table 2.2 Land and water interface results

Site	Years	Land (ha)	Water (ha)	Total (ha)	% Land	% Water
Cycle 5	4	67.6	24.7	92.3	73.2	26.8
Cycle 2	9	119.3	18.7	138.0	86.5	13.5
Cycle 3	12	80.9	12.7	93.6	86.4	13.6
Cycle 1	17	102.9	4.9	107.7	95.5	4.5
Reference North		44.8	4.5	49.2	91	9
Reference South		61.0	5.4	66.4	91.8	8.2

Table 2.3 Land and water calculations from drone imagery (June/July 2019), color infrared aerial photographs (7 December 2015), and WorldView-3 satellite imagery (13 February 2016)

Site	Total Area (ha)	Land (ha)	Water (ha)	% Land	% Water
Cycle 5 UAS (2019)	91.3	66.6	24.7	73	27
Cycle 5 Aerial Photo (2015)	93.9	59.9	34.0	63.8	36.2
Cycle 5 Satellite (2016)	94.2	27.1	67.08	28.8	71.2
Cycle 2 UAS (2019)	90.1	76.1	14.0	84.5	15.5
Cycle 2 Aerial Photo (2015)	91.1	70.4	20.6	77.3	22.7
Cycle 2 Satellite (2016)	92.6	74.5	18.1	80.4	19.6
Cycle 3 UAS (2019)	90.5	77.9	12.6	86.1	13.9
Cycle 3 Aerial Photo (2015)	90.2	88.2	2.0	97.8	2.2
Cycle 3 Satellite (2016)	95.2	89.6	5.6	94.1	5.9
Cycle 1 UAS (2019)	93.7	89.2	4.5	95.2	4.8
Cycle 1 Aerial Photo (2015)	96.7	91.1	5.7	94.1	5.9
Cycle 1 Satellite (2016)	94.4	90.1	4.2	95.5	4.5

Table 2.4 2019 Drone-based edge habitat calculations (marsh to water border)

Site	Years	Total Edge (km)	Interior (km)	Exterior (km)	Interior/Exterior Ratio
Cycle 5	4	64.1	54.3	9.8	5.5
Cycle 2	9	153.8	134.4	19.3	7
Cycle 3	12	104	92.2	11.7	7.9
Cycle 1	17	61.4	46.2	15.1	3.1
Reference North		56.9	45.2	11.7	3.9
Reference South		67.1	51.7	15.4	3.4

Table 2.5 Landscape metrics for land and water classes (water rows shown in gray)

Site	Class	Class Area (ha)	Percentage of Landscape	Number of Patches	Patch Density (#/100 ha)	Edge Density (m/ha)	Aggregation Index
Cycle 5	Land	67.6	73.2	648	718	575	99.9
Cycle 5	Water	24.7	26.8	795	880	575	99.7
Cycle 2	Land	119.3	86.5	730	529	954	99.8
Cycle 2	Water	18.7	13.5	4414	3199	954	99.1
Cycle 3	Land	80.9	86.4	5812	6212	862	99.9
Cycle 3	Water	12.7	13.6	723	773	862	99.2
Cycle 1	Land	102.9	95.5	181	168	423	99.9
Cycle 1	Water	4.9	4.5	469	435	423	98.8
Reference North	Land	44.8	91	659	1339	904	99.9
Reference North	Water	4.5	9	653	1327	904	98.8
Reference South	Land	61.0	91.8	1299	1957	768	99.9
Reference South	Water	5.4	8.2	342	515	768	98.8

Table 2.6 Landscape metrics for Cycle 2 run separately for the area within the original containment dikes and the overflow area (refer to figure 2.1 for delineation)

Site	Class	Class Area (ha)	Percentage of Landscape	Number of Patches	Patch Density	Edge Density	Aggregation Index
Cycle 2	Land	78.4	84.6	106	114	447	99.9
Cycle 2	Water	14.3	15.4	198	214	447	99.7
Cycle 2 Overflow	Land	41	90.5	652	1440	1993	99.7
Cycle 2 Overflow	Water	4.3	9.5	4200	9277	1993	97.4

Table 2.7 Class area statistics for 2019 drone-based classifications

Site	Class	Class Area (m ²)	Class Area (ha)	Total Area (ha)	Percent Cover (%)
Cycle 5	Bare ground	2588	0.3	92.3	0.3
Cycle 5	<i>D. spicata/S. patens</i>	77215	7.7	92.3	8.4
Cycle 5	<i>Phragmites australis</i>	3767	0.4	92.3	0.4
Cycle 5	<i>Spartina alterniflora</i>	589498	58.9	92.3	63.9
Cycle 5	Scrub shrub	2815	0.3	92.3	0.3
Cycle 5	Water	247252	24.7	92.3	26.8
Cycle 2	Bare ground	10935	1.1	137.9	0.8
Cycle 2	<i>D. spicata/S. patens</i>	120696	12.1	137.9	8.8
Cycle 2	<i>Phragmites australis</i>	3944	0.4	137.9	0.3
Cycle 2	<i>Spartina alterniflora</i>	1046735	104.7	137.9	75.9
Cycle 2	Scrub shrub	10263	1.0	137.9	0.7
Cycle 2	Water	186413	18.6	137.9	13.5
Cycle 3	Bare ground	1240	0.1	93.6	0.1
Cycle 3	<i>D. spicata/S. patens</i>	499193	49.9	93.6	53.4
Cycle 3	<i>Phragmites australis</i>	13996	1.4	93.6	1.5
Cycle 3	<i>Spartina alterniflora</i>	288088	28.8	93.6	30.8
Cycle 3	Scrub shrub	5922	0.6	93.6	0.6
Cycle 3	Water	127140	12.7	93.6	13.6
Cycle 1	Bare ground	6196	0.6	107.7	0.6
Cycle 1	<i>D. spicata/S. patens</i>	571781	57.2	107.7	53.1
Cycle 1	<i>Phragmites australis</i>	32161	3.2	107.7	3
Cycle 1	<i>Spartina alterniflora</i>	392380	39.2	107.7	36.4
Cycle 1	Scrub shrub	26280	2.6	107.7	2.4
Cycle 1	Water	48445	4.8	107.7	4.5
Reference North	<i>Eleocharis spp.</i>	9832	1.0	49.2	2
Reference North	Other	22830	2.3	49.2	4.6
Reference North	<i>Phragmites australis</i>	7130	0.7	49.2	1.5
Reference North	<i>Spartina alterniflora</i>	68594	6.9	49.2	13.9
Reference North	<i>Spartina patens</i>	331615	33.2	49.2	67.4
Reference North	Scrub shrub	7640	0.8	49.2	1.6
Reference North	Water	44619	4.5	49.2	9.1
Reference South	Other	64972	6.5	66.4	9.8
Reference South	<i>Phragmites australis</i>	20326	2.0	66.4	3.1
Reference South	<i>Spartina patens</i>	519549	52.0	66.4	78.2
Reference South	Scrub shrub	4816	0.5	66.4	0.7
Reference South	Water	54252	5.4	66.4	8.2

Table 2.8 Cycle 5 accuracy assessment (confusion) matrix results

Class	Bare ground	<i>D. spicata</i> <i>/S. patens</i>	<i>Phragmites</i> <i>australis</i>	<i>Spartina</i> <i>alterniflora</i>	Scrub shrub	Water	Total	U_Accuracy	Kappa
Bare ground	10	0	0	0	0	0	10	100%	0
<i>D. spicata/S. patens</i>	0	23	0	19	1	0	43	53%	0
<i>Phragmites australis</i>	0	0	10	0	0	0	10	100%	0
<i>Spartina alterniflora</i>	0	19	0	307	0	0	326	94%	0
Scrub shrub	0	0	0	6	4	0	10	40%	0
Water	1	0	0	5	0	120	126	95%	0
Total	11	42	10	337	5	120	525	0%	0
P_Accuracy	91%	55%	100%	91%	80%	100%	0	90%	0
Kappa	0	0	0	0	0	0	0	0	0.82

Table 2.9 Cycle 2 accuracy assessment (confusion) matrix results

Class	Bare ground	<i>D. spicata</i> <i>/S. patens</i>	<i>Phragmites</i> <i>australis</i>	<i>Spartina</i> <i>alterniflora</i>	Scrub shrub	Water	Total	U_Accuracy	Kappa
Bare ground	10	0	0	0	0	0	10	100%	0
<i>D. spicata/S. patens</i>	0	13	0	30	1	0	44	30%	0
<i>Phragmites australis</i>	0	0	8	0	1	1	10	80%	0
<i>Spartina alterniflora</i>	1	7	0	370	1	0	379	98%	0
Scrub shrub	0	2	0	5	3	0	10	30%	0
Water	0	0	0	4	0	64	68	94%	0
Total	11	22	8	409	6	65	521	0%	0
P_Accuracy	91%	59%	100%	90%	50%	98%	0	90%	0
Kappa	0	0	0	0	0	0	0	0	0.75

Table 2.10 Cycle 3 accuracy assessment (confusion) matrix results

Class	Bare ground	<i>D. spicata</i> / <i>S. patens</i>	<i>Phragmites australis</i>	<i>Spartina alterniflora</i>	Scrub shrub	Water	Total	U_Accuracy	Kappa
Bare ground	1	8	1	0	0	0	10	10%	0
<i>D. spicata</i> / <i>S. patens</i>	0	239	0	28	0	0	267	90%	0
<i>Phragmites australis</i>	0	1	7	1	1	0	10	70%	0
<i>Spartina alterniflora</i>	0	20	0	134	0	0	154	87%	0
Scrub shrub	0	2	1	0	7	0	10	70%	0
Water	0	1	0	8	0	59	68	87%	0
Total	1	271	9	171	8	59	519	0%	0
P_Accuracy	100%	88%	78%	78%	88%	100%	0	86%	0
Kappa	0	0	0	0	0	0	0	0	0.78

Table 2.11 Cycle 1 accuracy assessment (confusion) matrix results

Class	Bare ground	<i>D. spicata</i> <i>/S. patens</i>	<i>Phragmites australis</i>	<i>Spartina alterniflora</i>	Scrub shrub	Water	Total	U_Accuracy	Kappa
Bare ground	9	0	1	0	0	0	10	90%	0
<i>D. spicata/S. patens</i>	1	220	1	42	0	1	265	83%	0
<i>Phragmites australis</i>	0	2	13	0	0	0	15	87%	0
<i>Spartina alterniflora</i>	0	70	0	112	0	0	182	62%	0
Scrub shrub	0	4	0	1	7	0	12	58%	0
Water	0	0	0	2	0	20	22	91%	0
Total	10	296	15	157	7	21	506	0%	0
P_Accuracy	90%	74%	87%	71%	100%	95%	0	75%	0
Kappa	0	0	0	0	0	0	0	0	0.57

Table 2.12 Reference North accuracy assessment (confusion) matrix results

Class	<i>Eleocharis spp.</i>	Other	<i>Phragmites australis</i>	<i>Spartina alterniflora</i>	<i>Spartina patens</i>	Scrub shrub	Water	Total	U_Accuracy	Kappa
<i>Eleocharis spp.</i>	2	0	0	4	4	0	0	10	20%	0
Other	0	4	0	8	10	0	1	23	17%	0
<i>Phragmites australis</i>	0	0	8	0	2	0	0	10	80%	0
<i>Spartina alterniflora</i>	1	0	0	55	14	0	0	70	79%	0
<i>Spartina patens</i>	3	0	0	38	294	0	2	337	87%	0
Scrub shrub	0	0	0	3	7	0	0	10	0%	0
Water	1	0	0	3	0	0	41	45	91%	0
Total	7	4	8	111	331	0	44	505	0%	0
P_Accuracy	29%	100%	100%	50%	89%	0%	93%	0	80%	0
Kappa	0	0	0	0	0	0	0	0	0	0.62

Table 2.13 Reference South accuracy assessment (confusion) matrix results

Class	Other	<i>Phragmites australis</i>	<i>Spartina patens</i>	Scrub shrub	Water	Total	U_Accuracy	Kappa
Other	26	1	21	1	0	49	53%	0
<i>Phragmites australis</i>	0	15	0	0	0	15	100%	0
<i>Spartina patens</i>	74	0	312	2	3	391	80%	0
Scrub shrub	5	0	1	4	0	10	40%	0
Water	0	0	0	0	41	41	100%	0
Total	105	16	334	7	44	506	0%	0
P_Accuracy	25%	94%	93%	57%	93%	0	79%	0
Kappa	0	0	0	0	0	0	0	0.54

Figures

Figure 2.1 Location of study sites (Cycles) with final construction year in the Sabine National Wildlife Refuge (Bing 2017 base map)

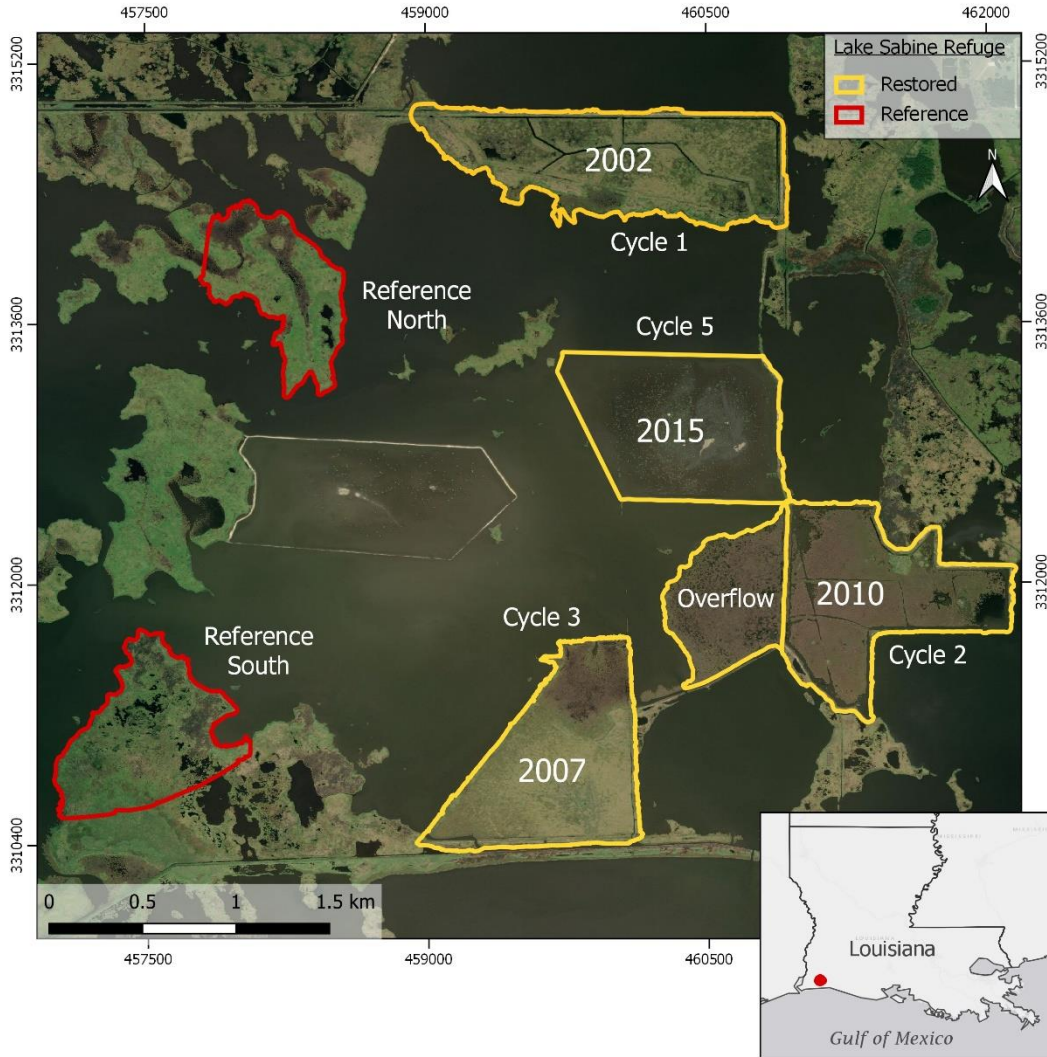


Figure 2.2 Field sampling locations and flight areas covered by the Yuneec H520. Examples of vegetation include: a mixture of *Spartina alterniflora*, *Schoenoplectus robustus*, and *Distichlis spicata* in the foreground with taller *Phragmites australis* in the background (a) and *Spartina alterniflora* (b)

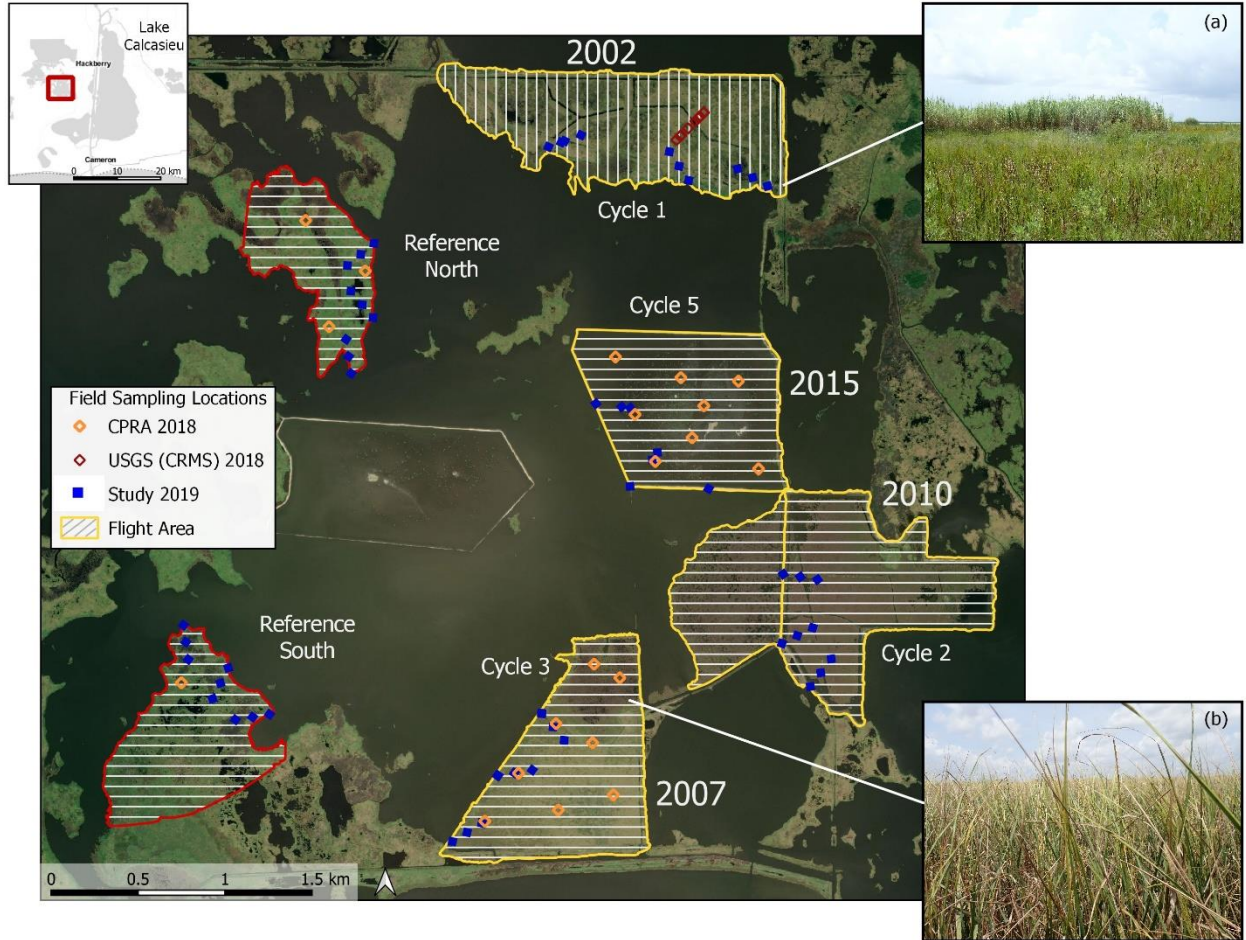


Figure 2.3 Data products from June 2019 drone imagery for Cycle 3 including: orthomosaic (a), digital surface model (b), land water interface (c), and vegetation classification (d)

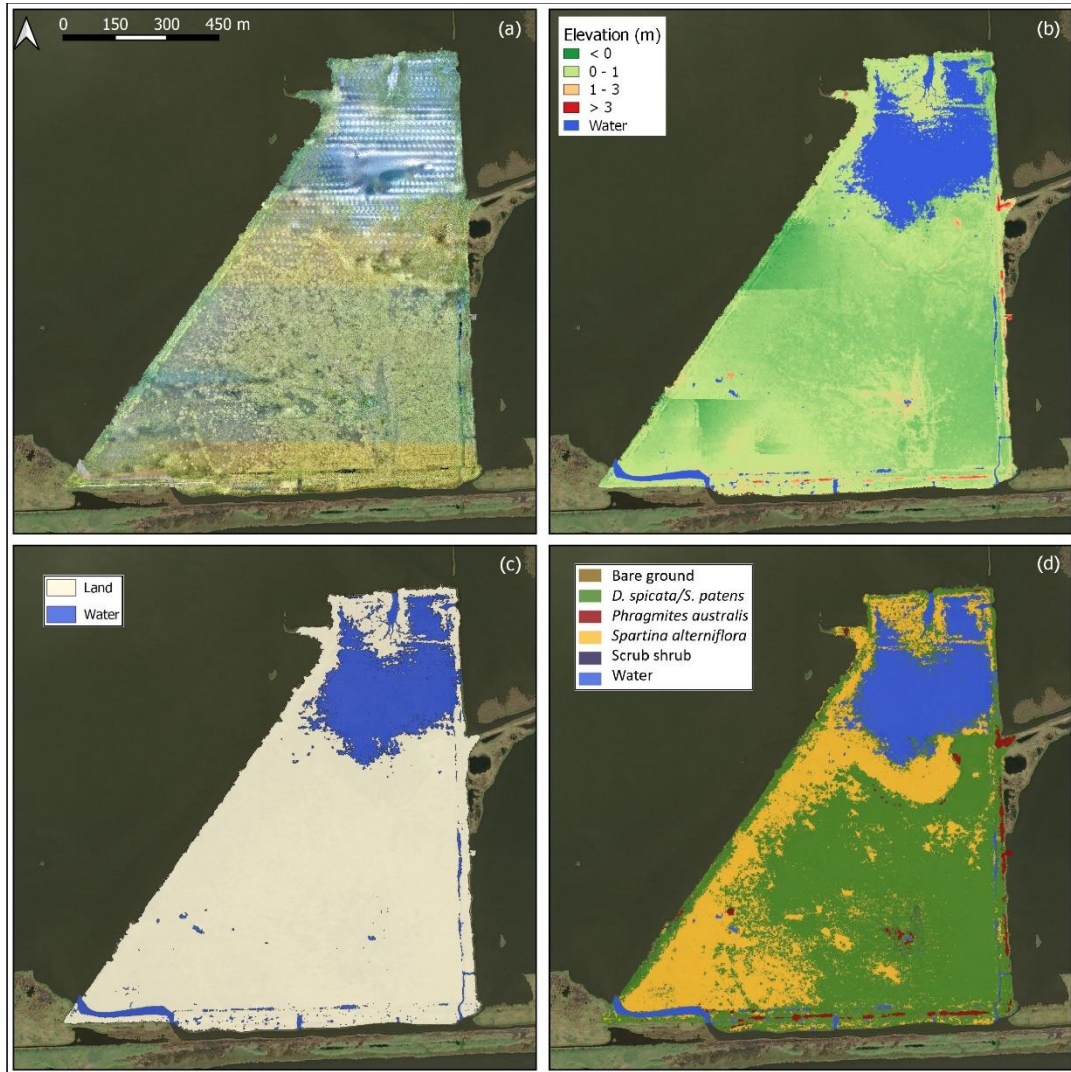


Figure 2.4 Workflow for obtaining, processing, and analyzing drone imagery

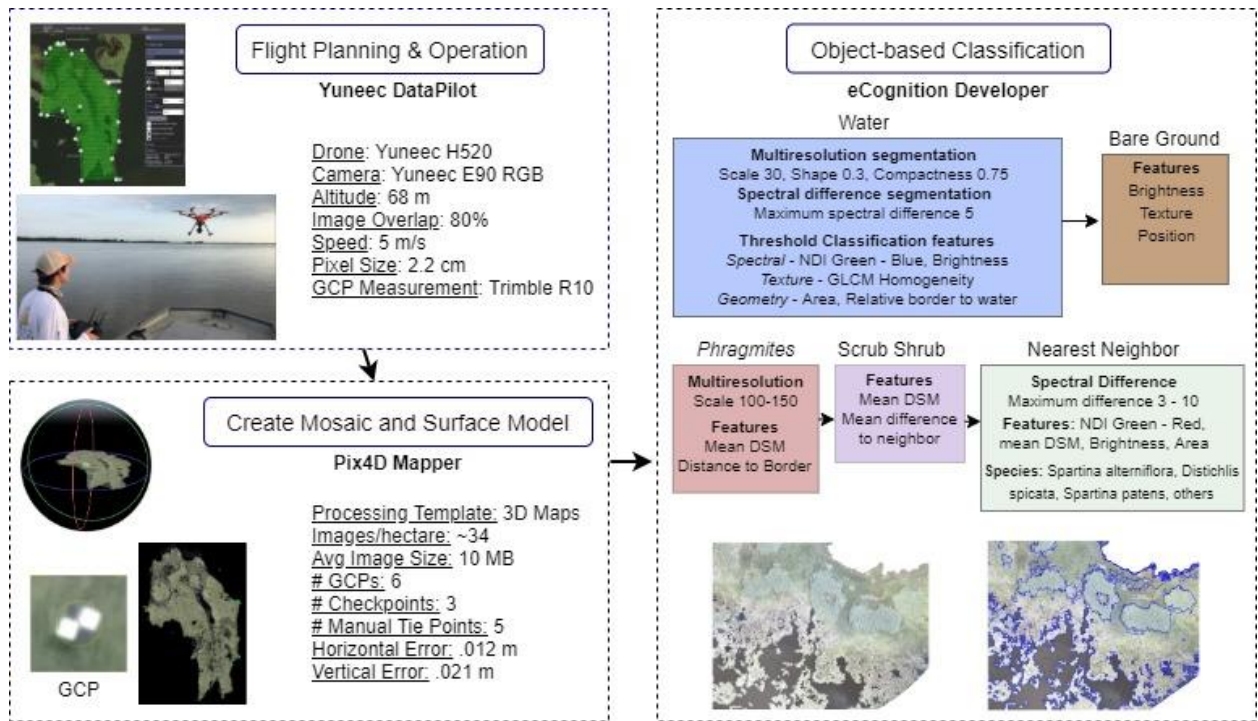


Figure 2.5 Example of *Spartina patens* marsh illustrating an aggregated piece of habitat (a) (AI = 100) and a less aggregated piece of habitat (b) (AI = 99)

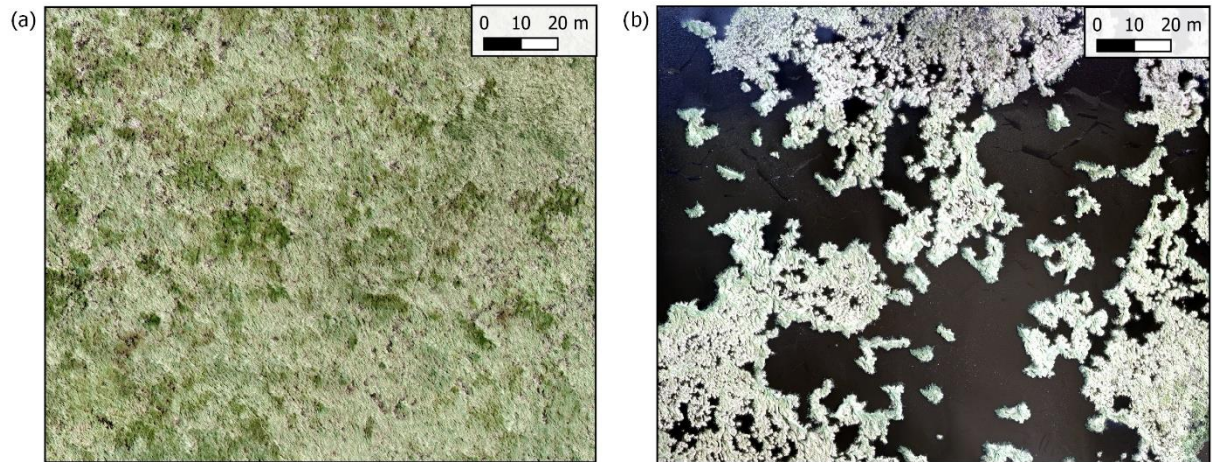


Figure 2.6 Summer 2019 drone-based percent land cover for restored sites over time since restoration (gray area is 95% confidence interval for logarithmic line)

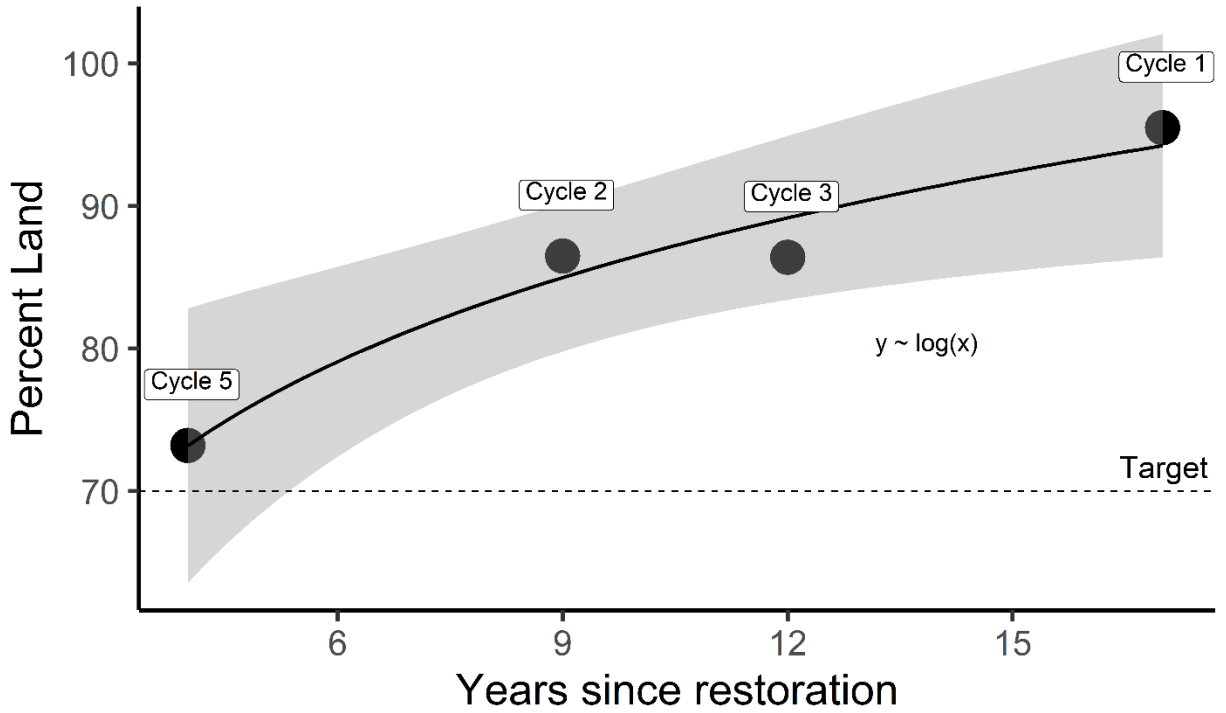


Figure 2.7 Summer 2019 drone-based land and water interface maps (years since construction as of 2019) (Bing 2017 base map)



Figure 2.8 Summer 2019 drone-based vegetation classification maps (years since construction as of 2019) (Bing 2017 base map)

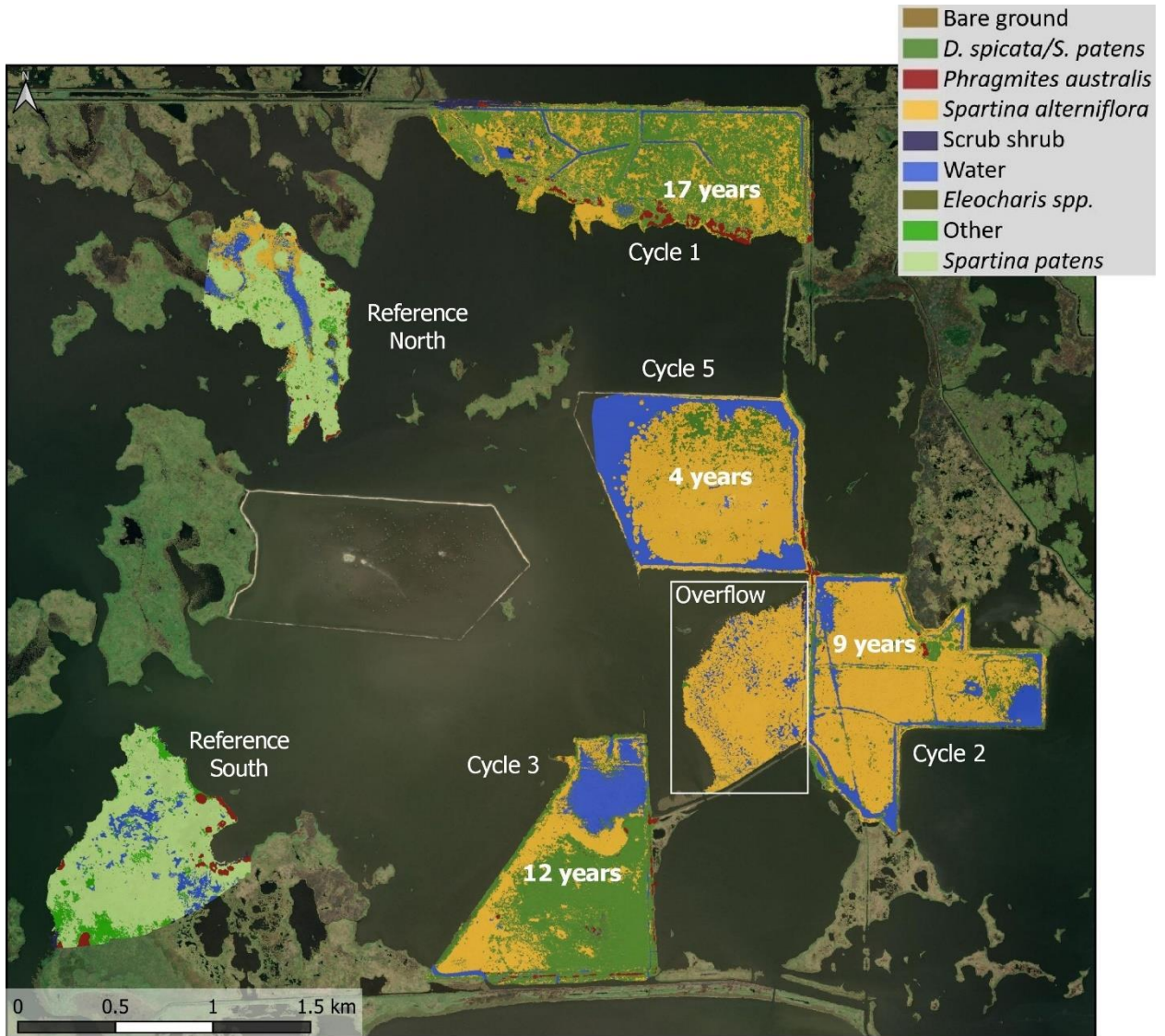


Figure 2.9 Drone-based percent cover calculations by species and land cover class

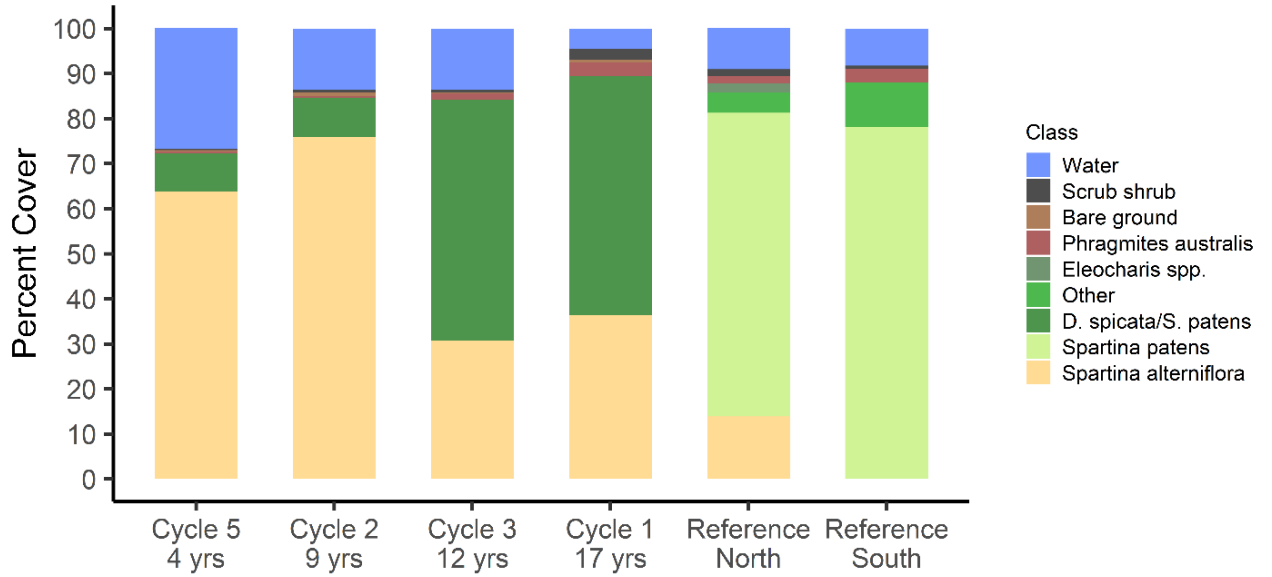


Figure 2.10 July 2019 Cycle 5 (4 years old) orthomosaic (a) with zoomed in portions (b) and corresponding classifications (c)

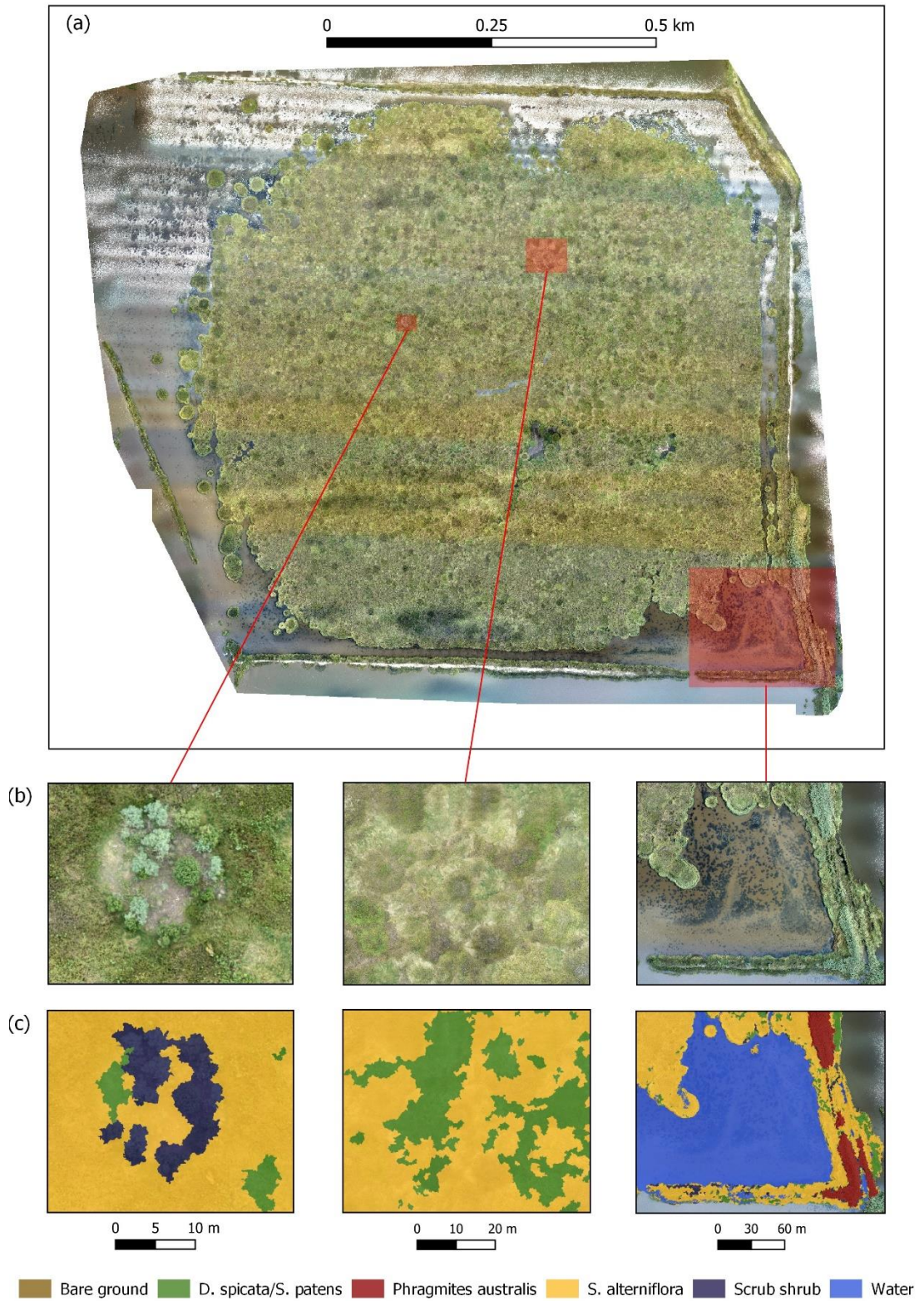


Figure 2.11 July 2019 Cycle 2 (9 years old) orthomosaic (a) with zoomed in view of the overflow area (b) and corresponding classification (c) to highlight the detail of drone products and the tidal channels and edge habitat created by the overflow technique

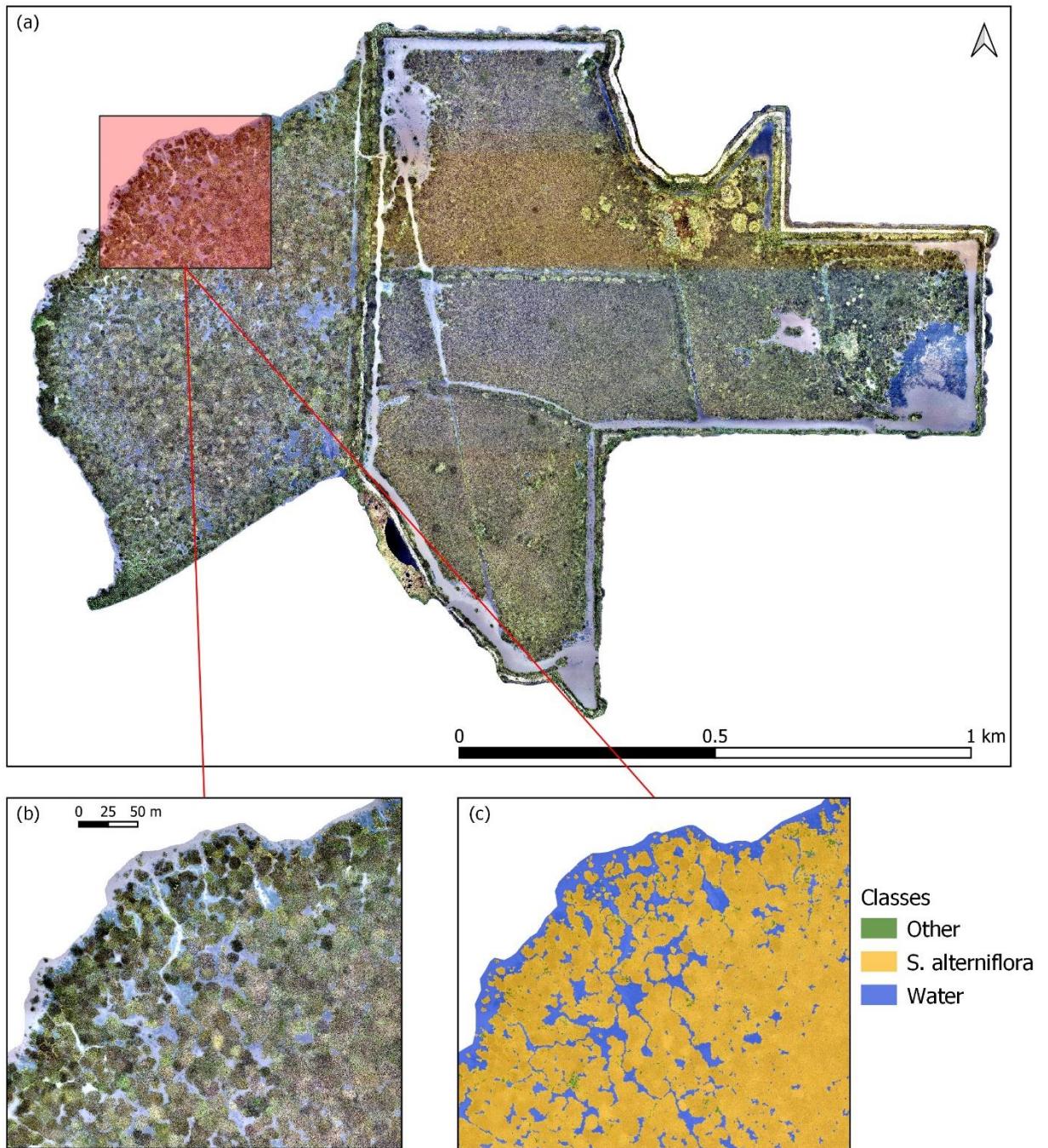


Figure 2.12 June 2019 Cycle 3 (12 years old) orthomosaic (a) and classification (b) with zoomed in view of the flooded portion (c) and corresponding classification (d)

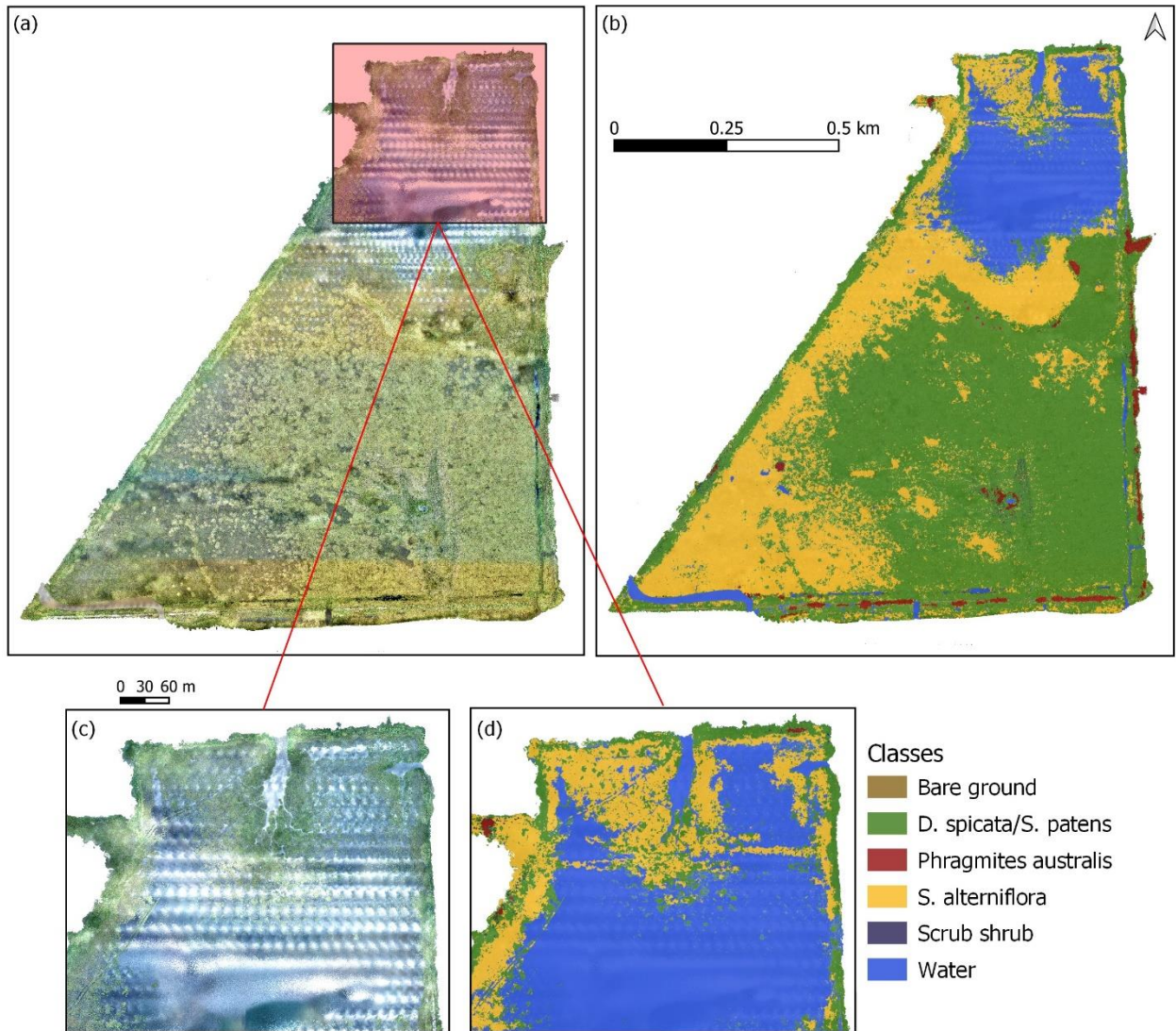


Figure 2.13 June 2019 Cycle 1 (17 years old) orthomosaic (a) and corresponding classification map (b) with zoomed in portions highlighting *Phragmites australis* (c) and portion of man-made channel filling in (d)

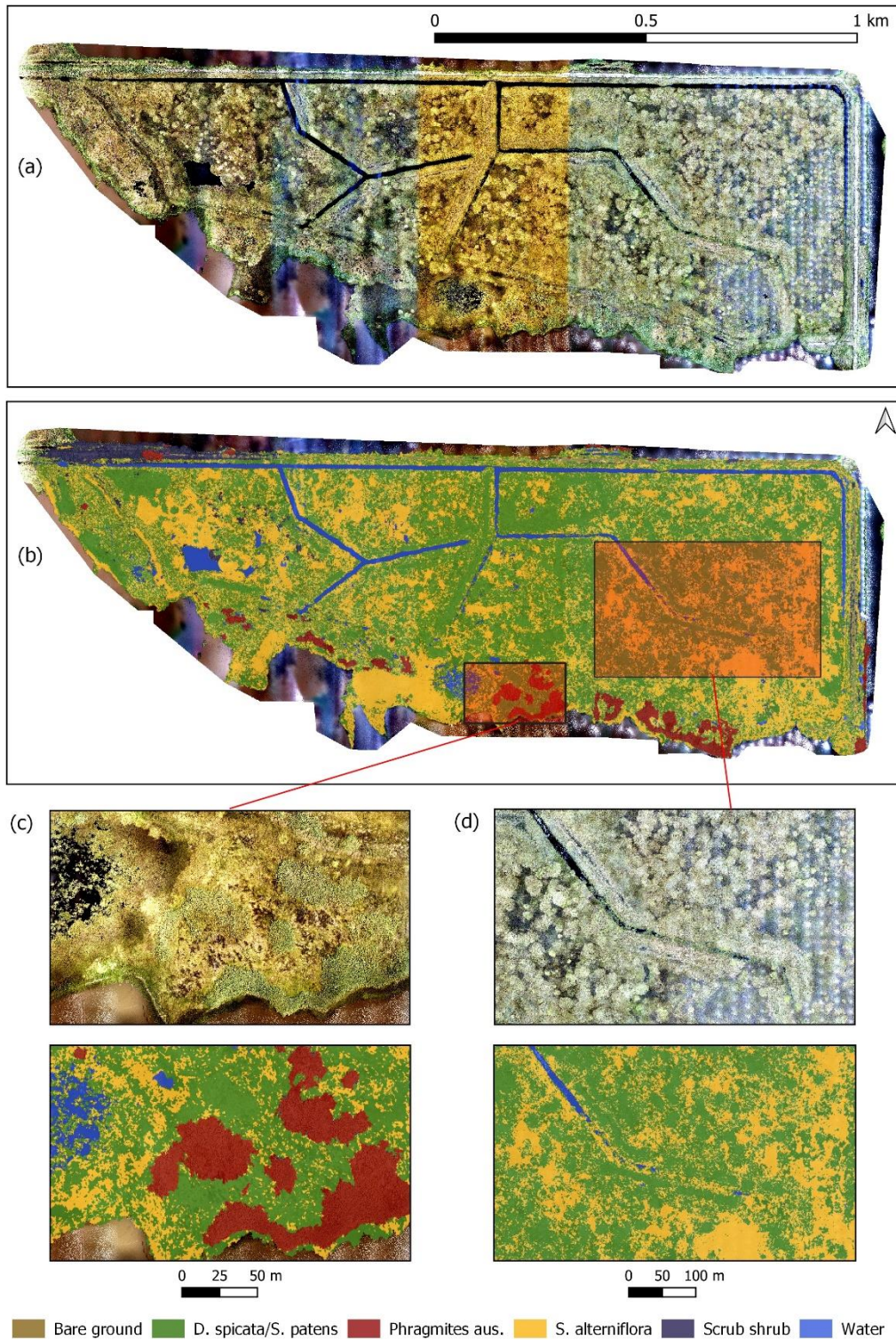


Figure 2.14 June 2019 Reference North orthomosaic (a) with corresponding classification (b) and Reference South orthomosaic (c) with corresponding classification (d)

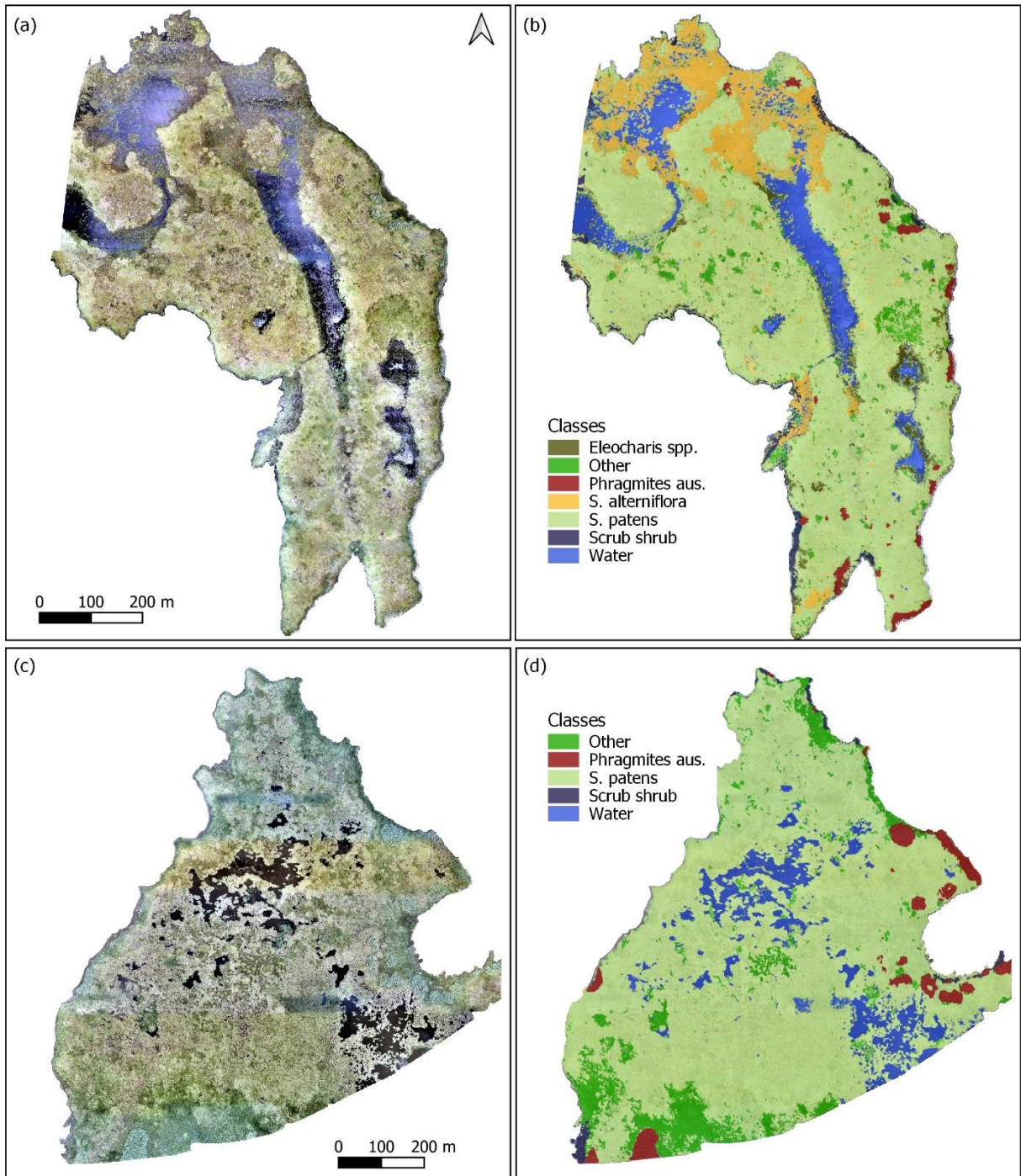


Figure 2.15 2019 field-based percent vegetation cover estimates

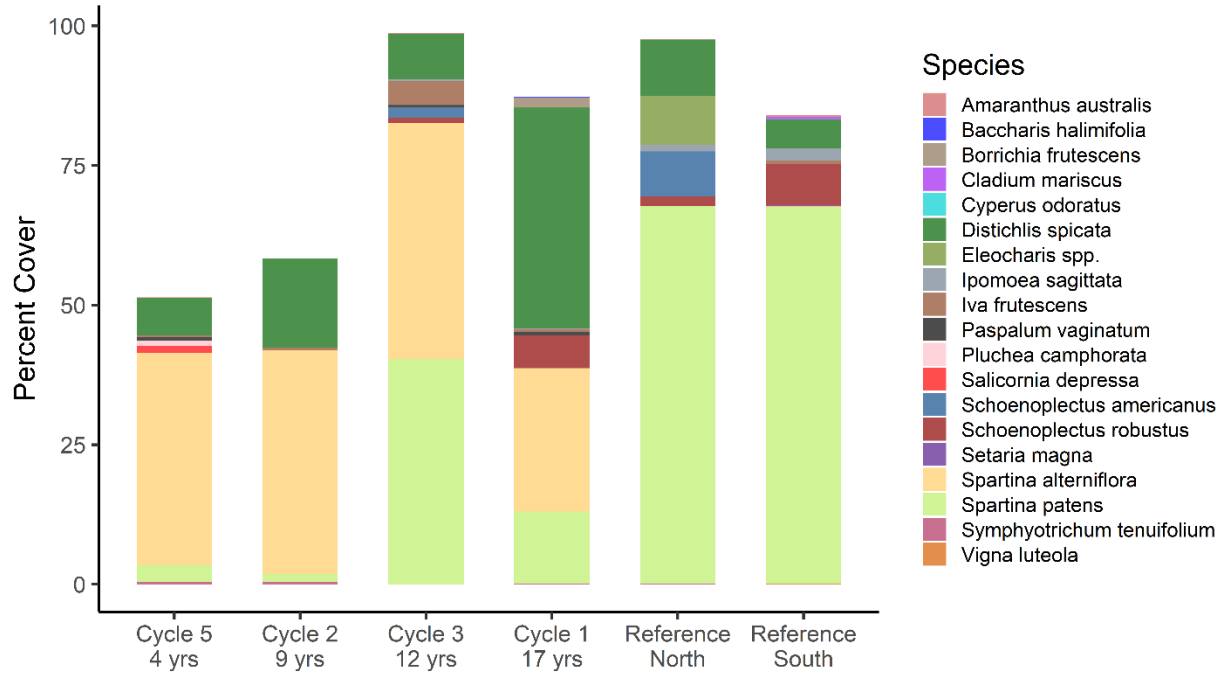


Figure 2.16 Field-based species richness (a) (# species per plot) (ANOVA, $F_{5,49} = 2.01$, $P = .0941$) and average percent vegetated cover estimates (b) (ANOVA, $F_{5,49} = 6.28$, $P = .0001$)

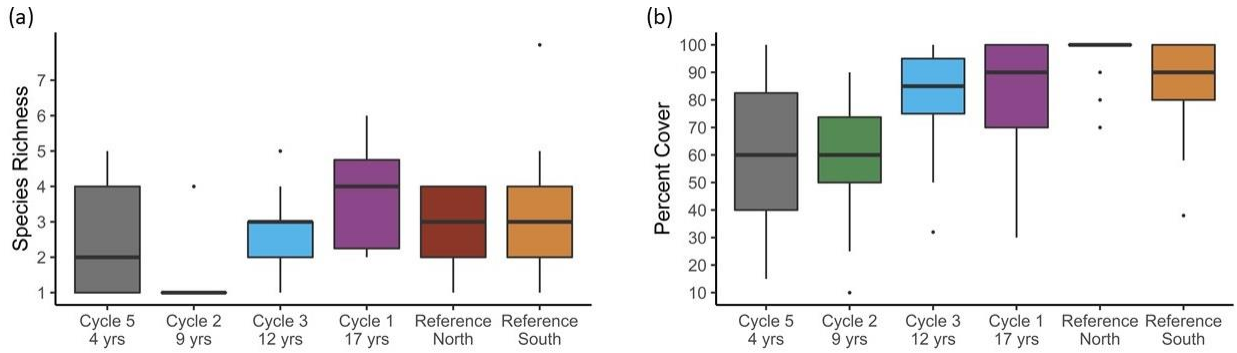


Figure 2.17 2019 field-based Floristic Quality Index (FQI) scores

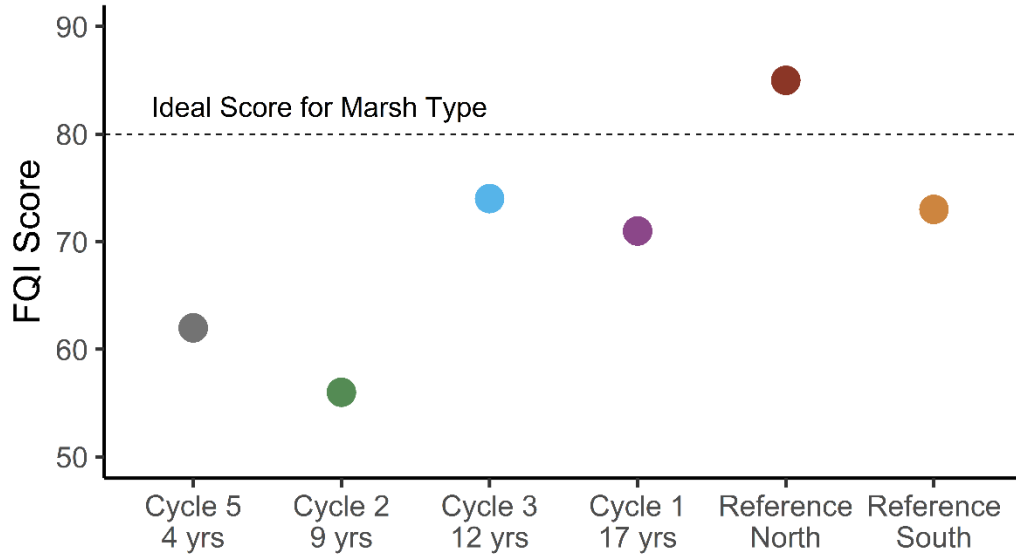


Figure 2.18 Dominant cover type comparison of 2018 state agency field surveys (Agency) and 2019 drone-based classifications (Drone) and field surveys (Field). Classes grouped into high marsh (*D. spicata* and *S. patens*), low marsh (*S. alterniflora*), and other (all other species) for general comparison across data types. Agency and Field columns based on visual percent cover estimates from plot surveys

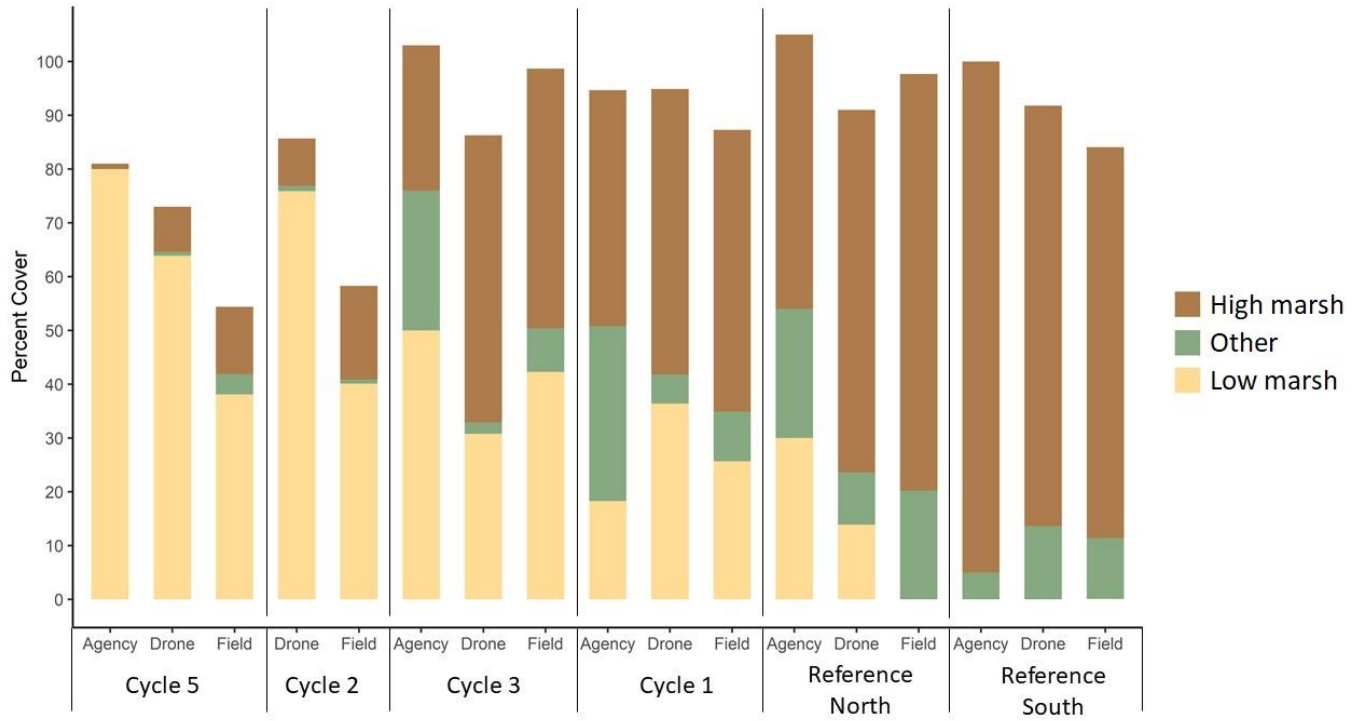


Figure 2.19 Standardized edge habitat comparison (edge considered marsh to water border)

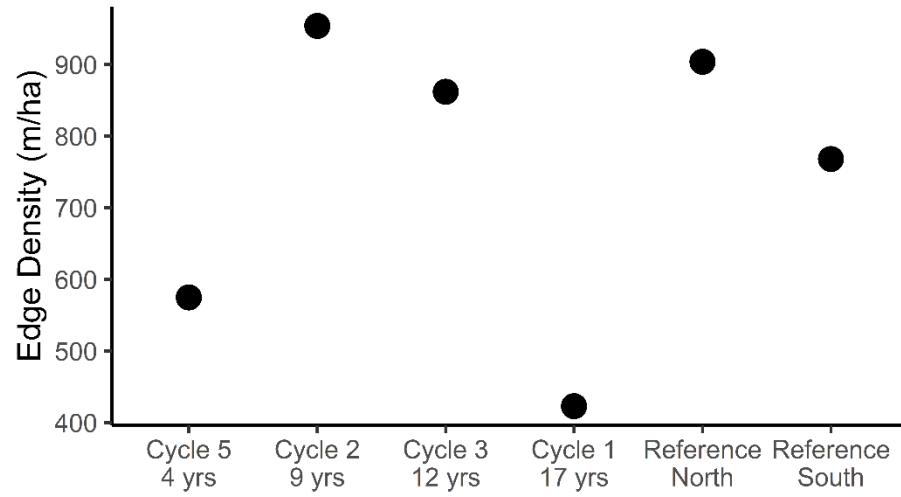
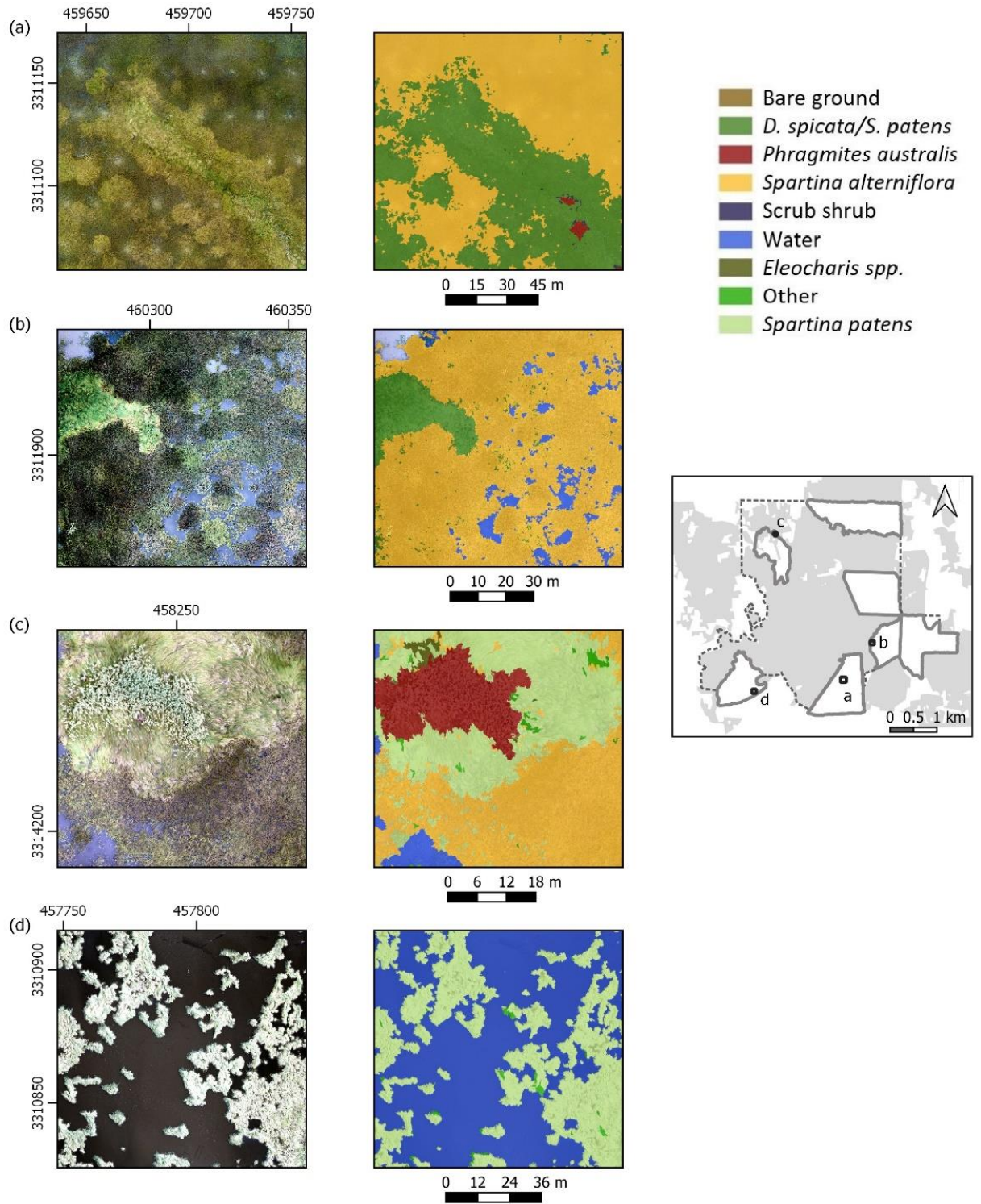


Figure 2.20 Orthomosaic (left) and corresponding vegetation classification (right) at study sites: Cycle 3 (a), Cycle 2 (b), Reference North (c), and Reference South (d)



References

- Anderson K, Gaston KJ (2013) Lightweight unmanned aerial vehicles will revolutionize spatial ecology. *Frontiers in Ecology and the Environment* 11:138–146
- Baatz M, Schäpe A (2000) Multiresolution segmentation: an optimization approach for high quality multi-scale image segmentation. *Angewandte Geographische Informationsverarbeitung XII*:12–23
- Barras JA, Bernier JC, Morton RA (2008) Land change in coastal Louisiana: A multidecadal perspective (from 1956 - 2006). U.S. Geological Survey Scientific Investigations Map 3019, Reston, VA
- Beck HJ et al. (2019) Sabine Refuge Marsh Creation (CS-28): Coastal wetlands planning, protection and restoration act 2015 land-water classification. U.S. Geological Survey
- Bell SS, Fonseca MS, Motten LB (1997) Linking restoration and landscape ecology. *Restoration Ecology* 5:318–323
- Bernier JC, Morton RA, Kelso KW (2011) Trends and causes of historical wetland loss, Sabine National Wildlife Refuge, Southwest Louisiana. U.S. Geological Survey Open-File Report 1169, Reston, VA
- Bertness MD (1991) Zonation of *Spartina patens* and *Spartina alterniflora* in New England salt marsh. *Ecology* 72:138–148
- Blaschke T (2009) Object based image analysis for remote sensing. *ISPRS Journal of Photogrammetry and Remote Sensing* 65:2–16
- Bradshaw AD (1996) Underlying principles of restoration. *Canadian Journal of Fisheries and Aquatic Sciences* 53:3–9
- Broome SW, Craft CB, Burchell MR (2019) Tidal Marsh Creation. In: Coastal wetlands: an integrated ecosystem approach. Perillo, GME, Wolanski, E, Cahoon, DR, & Hopkinson, CS, editors. Elsevier pp. 789–816.
- Broussard W, Suir G, Visser J (2018) Unmanned Aircraft Systems (UAS) and satellite imagery collections in a coastal intermediate marsh to determine the land-water interface, vegetation types, and normalized difference vegetation index (NDVI) values. U.S. Army Engineer Research and Development Center. ERDC/TN WRAP-18-1, Vicksburg, MS
- Chapple D, Dronova I (2017) Vegetation development in a tidal marsh restoration project during a historic drought. *Frontiers in Marine Science* 4:1–12
- Christie KS et al. (2016) Unmanned aircraft systems in wildlife research: current and future applications of a transformative technology. *Frontiers in Ecology and the Environment* 14:241–251

- Coastal Protection and Restoration Authority of Louisiana (CPRA) (2020) Coastwide Reference Monitoring System-Wetlands Monitoring Data. Coastal Information Management System (CIMS) database (accessed 25 June 2020)
- Congalton RG (1991) A review of assessing the accuracy of classifications of remotely sensed data. *Remote Sensing of Environment* 37:35–46
- Couvillion BR et al. (2016) Spatial configuration trends in coastal Louisiana from 1985 to 2010. *Wetlands* 36:347–359
- Cowardin LM et al. (1979) Classification of wetlands and deepwater habitats of the United States. U.S. Department of the Interior, Fish and Wildlife Service FWS/OBS-79/31, Washington, D.C.
- Craft C, Broome S, Campbell C (2002) Fifteen years of vegetation and soil development after brackish-water marsh creation. *Restoration Ecology* 10:248–258
- Craft C et al. (1999) Twenty-five years of ecosystem development of constructed *Spartina alterniflora* (loisel) marshes. *Ecological Applications* 9:1405–1419
- Cretini KF et al. (2011) Development and use of a floristic quality index for coastal Louisiana marshes. *Environmental Monitoring and Assessment* 184:2389–2403
- Dronova I (2015) Object-based image analysis in wetland research: a review. *Remote Sensing* 7:6380–6413
- Folse TM et al. (2014) A standard operating procedures manual for the coastwide reference monitoring system - wetlands: methods for site establishment, data collection, and quality assurance/quality control. Louisiana Coastal Protection and Restoration Authority (CPRA), Baton Rouge, LA
- Forsmoo J et al. (2019) Structure from motion photogrammetry in ecology: Does the choice of software matter? *Ecology and Evolution* 9:12964–12979
- Gann GD et al. (2019) International principles and standards for the practice of ecological restoration. *Restoration Ecology* 27:1–99
- Gianopoulos K (2014) Coefficient of conservatism database development for wetland plants occurring in the southeastern United States. North Carolina Dept. of Environment & Natural Resources, Division of Water Resources: Wetlands Branch
- He HS, DeZonia BE, Mladenoff DJ (2000) An aggregation index (AI) to quantify spatial patterns of landscapes. *Landscape Ecology* 15:591–601
- Hesselbarth MHK et al. (2019) Landscape metrics for categorical map patterns. *Ecography* 42:1648-1657(ver. 0)

- Hossain MD, Chen D (2019) Segmentation for object-based image analysis (OBIA): A review of algorithms and challenges from remote sensing perspective. *ISPRS Journal of Photogrammetry and Remote Sensing* 150:115–134
- Hunt ER et al. (2005) Evaluation of digital photography from model aircraft for remote sensing of crop biomass and nitrogen status. *Precision Agriculture* 6:359–378
- Husson E, Ecke F, Reese H (2016) Comparison of manual mapping and automated object-based image analysis of non-submerged aquatic vegetation from very-high-resolution UAS images. *Remote Sensing* 8:1–18
- Jackson LL, Lopoukhine N, Hillyard D (1995) Ecological restoration: a definition and comments. *Restoration Ecology* 3:71–75
- Kelly M, Tuxen KA, Stralberg D (2011) Mapping changes to vegetation pattern in a restoring wetland: Finding pattern metrics that are consistent across spatial scale and time. *Ecological Indicators* 11:263–273
- Kirwan ML et al. (2016) Overestimation of marsh vulnerability to sea level rise. *Nature Climate Change* 6:253–260
- Klemas V (2015) Coastal and environmental remote sensing from unmanned aerial vehicles: An overview. *Journal of Coastal Research* 31:1260–1267
- Klemas V (2013) Using remote sensing to select and monitor wetland restoration sites: An overview. *Journal of Coastal Research* 29:958–970
- Knoth C et al. (2013) Unmanned aerial vehicles as innovative remote sensing platforms for high-resolution infrared imagery to support restoration monitoring in cut-over bogs. *Applied Vegetation Science* 1–9
- Lake PS (2001) On the maturing of restoration: linking ecological research and restoration. *Ecological Management & Restoration* 2:110–115
- Laliberte AS, Rango A (2011) Image processing and classification procedures for analysis of sub-decimeter imagery acquired with unmanned aircraft over arid rangelands. *GIScience & Remote Sensing* 28:4–23
- Laliberte AS, Rango A (2009) Texture and scale in object-based analysis of subdecimeter resolution unmanned aerial vehicle (UAV) imagery. *IEEE Transactions on Geoscience and Remote Sensing* 47
- Liu AJ, Cameron GN (2001) Analysis of landscape patterns in coastal wetlands of Galveston Bay, Texas (USA). *Landscape Ecology* 16:581–595
- Lopez RD, Fennessy MS (2002) Testing the floristic quality assessment index as an indicator of wetland condition. *Ecological Applications* 12:487–497

- Louisiana Coastal Wetlands Conservation and Restoration Task Force (2018) Sabine marsh creation Cycles 6 & 7 (CS-81). Louisiana Coastal Protection and Restoration Authority
- Louisiana Coastal Wetlands Conservation and Restoration Task Force (2012) The 2012 evaluation report to the U.S. congress on the effectiveness of coastal wetlands planning, protection and restoration act projects.
- Manfreda S et al. (2019) Assessing the accuracy of digital surface models derived from optical imagery acquired with unmanned aerial systems. *Drones* 3:15
- McGarigal K (2015) FRAGSTATS help. Pieejams 1–182
- Middleton BA (1999) Wetland restoration, flood pulsing, and disturbance dynamics. John Wiley & Sons, New York, NY
- Miller M (2014) 2014 Operations, maintenance, and monitoring report for Sabine Refuge Marsh Creation (CS-28). Louisiana Coastal Protection and Restoration Authority
- Miller M, Guidry M, White J (2019) 2019 Short Summary Report: Sabine Refuge Marsh Creation Cycles - 3-4-5. Louisiana Coastal Protection and Restoration Authority
- Minello TJ, Zimmerman RJ, Medina R (1994) The importance of edge for natant macrofauna in a created salt marsh. *Wetlands* 14:184–198
- Morgan PA, Short FT (2002) Using functional trajectories to track constructed salt marsh development in the Great Bay Estuary, Maine/New Hampshire, U.S.A. *Restoration Ecology* 10:461–473
- Morris JT et al. (2002) Responses of coastal wetlands to rising sea level. *Ecology* 83:2869–2877
- Nelson JA et al. (in review) New mapping metrics to test functional response of food webs to coastal restoration. *Food Webs*
- Oniga V-E, Breaban A-I, Statescu F (2018) Determining the optimum number of ground control points for obtaining high precision results based on UAS images. *Proceedings* 2:352
- Pajares G (2015) Overview and current status of remote sensing applications based on unmanned aerial vehicles (UAVs). *Photogrammetric Engineering & Remote Sensing* 81:281–330
- Palmer MA, Ambrose RF, Poff NL (1997) Ecological theory and community restoration ecology. *Restoration Ecology* 5:291–300

- Pande-Chhetri R et al. (2017) Object-based classification of wetland vegetation using very high-resolution unmanned air system imagery. *European Journal of Remote Sensing* 50:564–576
- Patton BA, Nyman JA, Lapeyre MK (2020) Living on the edge: Multi-scale analyses of bird habitat use in coastal marshes of Barataria Basin, Louisiana, USA. *Wetlands*
- Pontiff DJ, White J (2017) 2016/2017 Annual Inspection Report: Sabine Refuge Marsh Creation Project (CS-28-4&5). Louisiana Coastal Protection and Restoration Authority
- Ridge JT, Johnston DW (2020) Unoccupied aircraft systems (UAS) for marine ecosystem restoration. *Frontiers in Marine Science* 7
- Samiappan S et al. (2016) Using unmanned aerial vehicles for high-resolution remote sensing to map invasive *Phragmites australis* in coastal wetlands. *International Journal of Remote Sensing* 38:2199–2217
- Sharp LA (2011) 2011 operations, maintenance, and monitoring report for Sabine Refuge Marsh Creation (CS-28). Louisiana Coastal Protection and Restoration Authority
- Shuman CS, Ambrose RF (2003) A comparison of remote sensing and ground-based methods for monitoring wetland restoration success. *Restoration Ecology* 11:325–333
- Simenstad C, Reed D, Ford M (2006) When is restoration not? Incorporating landscape-scale processes to restore self-sustaining ecosystems in coastal wetland restoration. *Ecological Engineering* 26:27–39
- Stagg CL et al. (2019) Quantifying hydrologic controls on local- and landscape-scale indicators of coastal wetland loss. *Annals of Botany* XX:1–12
- Suir G, Sasser C (2017) Floristic quality index of restored wetlands in coastal Louisiana. U.S. Army Engineer Research and Development Center. ERDC/EL TR-17-15, Vicksburg, MS
- Suir GM et al. (2013) Development of a reproducible method for determining quantity of water and its configuration in a marsh landscape. *Journal of Coastal Research* 63:110–117
- Suir GM et al. (2019) Comparing carbon accumulation in restored and natural wetland soils of coastal Louisiana. *International Journal of Sediment Research* 34:600–607
- Suir GM, Sasser CE, Harris JM (2020) Use of remote sensing and field data to quantify the performance of restored Louisiana wetlands. *Wetlands in revision*
- Taddeo S, Dronova I (2019) Landscape metrics of post-restoration vegetation dynamics in wetland ecosystems. *Landscape Ecology*

- Turner MG (1989) Landscape ecology: The effect of pattern on process. *Annual Review of Ecology and Systematics* 20:171–197
- Tuxen KA et al. (2008) Vegetation colonization in a restoring tidal marsh: A remote sensing approach. *Restoration Ecology* 16:313–323
- Wiens JA et al. (1993) Ecological mechanisms and landscape ecology. *Oikos* 66:369–380
- Woodget A et al. (2017) Unmanned aerial vehicles for environmental applications. *International Journal of Remote Sensing* 38:2029–2036
- Young TP, Chase JM, Huddleston RT (2001) Comparing, contrasting and combining paradigms in the context of ecological restoration. *Ecological Restoration* 19:5–18
- Zedler JB (2000) Progress in wetland restoration ecology. *Trends in Ecology & Evolution* 15:402–407

Harris, J. Mason. Bachelor of Arts, Sewanee: University of the South, Spring 2014; Master of Science, University of Louisiana at Lafayette, Summer 2020

Major: Biology

Title of Thesis: Evaluating Coastal Wetland Restoration in Louisiana Using Drones

Thesis Advisor: Dr. James Nelson

Pages in Thesis: 91; Words in Abstract: 197

Abstract

Coastal marsh ecosystems are disappearing rapidly in Louisiana. The state has undertaken massive wetland restoration efforts to preserve its coastal zone but traditional methods to monitor restoration success rely on labor intensive field measurements that are often short-term and underfunded. To address this, I developed methods using a commercially available drone with a high-resolution RGB camera to assess the effects of wetland restoration and integrate more modern tools into evaluation approaches. I conducted drone flights at restored brackish marshes of various ages using a space for time substitution to understand the ecological sequence of marsh creation. Created marshes had higher percentages of land than natural marshes after about 12 - 15 years and dominant species in created marshes shifted from *Spartina alterniflora* to *Distichlis spicata*, *Spartina patens*, and others after about 10 years while natural marshes were dominated by *S. patens*. Older sites were configured like reference areas based on some landscape metrics and indicators of fragmentation, but other indices reflected developmental differences possibly related to construction practices. Drone surveys offer low-cost, minimally invasive methods for evaluating restored wetlands and ultimately inform more about ecosystem development than traditional methods through the production of realistic site-level habitat configurations.

Biographical Sketch

Mason Harris was born and raised in Creedmoor, North Carolina. He graduated from Sewanee: University of the South in 2014 with a Bachelor of Arts in natural resources. He then entered the master's program in biology at UL Lafayette in 2018 and graduated in 2020.

ProQuest Number: 28085932

INFORMATION TO ALL USERS

The quality and completeness of this reproduction is dependent on the quality and completeness of the copy made available to ProQuest.



Distributed by ProQuest LLC (2021).

Copyright of the Dissertation is held by the Author unless otherwise noted.

This work may be used in accordance with the terms of the Creative Commons license or other rights statement, as indicated in the copyright statement or in the metadata associated with this work. Unless otherwise specified in the copyright statement or the metadata, all rights are reserved by the copyright holder.

This work is protected against unauthorized copying under Title 17, United States Code and other applicable copyright laws.

Microform Edition where available © ProQuest LLC. No reproduction or digitization of the Microform Edition is authorized without permission of ProQuest LLC.

ProQuest LLC
789 East Eisenhower Parkway
P.O. Box 1346
Ann Arbor, MI 48106 - 1346 USA